



January 2017

# Calibration Uncertainties In The Droplet Measurement Technologies Cloud Condensation Nuclei Counter

Kurt James Hibert

Follow this and additional works at: <https://commons.und.edu/theses>

---

## Recommended Citation

Hibert, Kurt James, "Calibration Uncertainties In The Droplet Measurement Technologies Cloud Condensation Nuclei Counter" (2017). *Theses and Dissertations*. 2231.  
<https://commons.und.edu/theses/2231>

This Thesis is brought to you for free and open access by the Theses, Dissertations, and Senior Projects at UND Scholarly Commons. It has been accepted for inclusion in Theses and Dissertations by an authorized administrator of UND Scholarly Commons. For more information, please contact [zeinebyousif@library.und.edu](mailto:zeinebyousif@library.und.edu).

CALIBRATION UNCERTAINTIES IN THE DROPLET MEASUREMENT TECHNOLOGIES  
CLOUD CONDENSATION NUCLEI COUNTER

by

Kurt James Hibert  
Bachelor of Science, University of North Carolina Asheville, 2014

A Thesis

Submitted to the Graduate Faculty

of the

University of North Dakota

in partial fulfillment of the requirements


for the degree of


Master of Science

Grand Forks, North Dakota

August  
2017

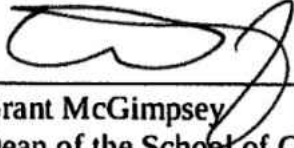
This thesis, submitted by Kurt James Hibert in partial fulfillment of the requirements for the Degree of Master of Science from the University of North Dakota, has been read by the Faculty Advisory Committee under whom the work has been done and is hereby approved.

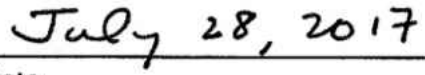
  
\_\_\_\_\_  
David Delene

  
\_\_\_\_\_  
Michael Poellot

  
\_\_\_\_\_  
Frank Bowman

This thesis is being submitted by the appointed advisory committee as having met all of the requirements of the School of Graduate Studies at the University of North Dakota and is hereby approved.

  
\_\_\_\_\_  
Grant McGimpsey  
Dean of the School of Graduate Studies

  
\_\_\_\_\_  
Date

## PERMISSION

Title            Calibration Uncertainties in the Droplet Measurement Technologies Cloud  
                    Condensation Nuclei Counter

Department    Atmospheric Sciences

Degree         Master of Science

In presenting this thesis in partial fulfillment of the requirements for a graduate degree from the University of North Dakota, I agree that the library of this University shall make it freely available for inspection. I further agree that permission for extensive copying for scholarly purposes may be granted by the professor who supervised my thesis work or, in his absence, by the Chairperson of the department or the dean of the School of Graduate Studies. It is understood that any copying or publication or other use of this thesis or part thereof for financial gain shall not be allowed without my written permission. It is also understood that due recognition shall be given to me and to the University of North Dakota in any scholarly use which may be made of any material in my thesis.

Kurt Hibert  
July 20<sup>th</sup>, 2017

## TABLE OF CONTENTS

LIST OF FIGURES.....	v
ABSTRACT.....	vi
CHAPTER	
I. INTRODUCTION.....	1
II. METHODOLOGY.....	9
III. DATA.....	23
IV. DISCUSSION.....	32
V. CONCLUSION.....	40
APPENDICES.....	42
REFERENCES.....	57

## LIST OF FIGURES

Figure	Page
1. Size Distribution of NaCl Aerosols.....	11
2. Ammonium Sulfate.....	12
3. Laboratory Setup.....	13
4. Flow Diagram of the DMA Main Cylinder.....	15
5. DMT CCN Counter (Serial Number 062) Pressure Calibration.....	23
6. DMT CCN Counter (Serial Number 062) Sheath Flow Calibration.....	24
7. DMT CCN Counter (Serial Number 062) Sample Flow Calibration.....	24
8. Activation curves for data taken at $\Delta T$ of 6 and 14 K on October 28 <sup>th</sup> , 2016.....	25
9. 980 hPa Supersaturation Calibrations.....	27
10. 840 hPa Supersaturation Calibrations.....	29
11. 700 hPa Supersaturation Calibrations.....	29
12. Supersaturation pressure dependence.....	30
13. Supersaturation pressure dependence with $\Delta T$ .....	31
14. Supersaturation Spectra of Outdoor Air.....	34
15. Supersaturation calibrations done at 840 hPa.....	36
16. Comparison of Köhler theory used by UND and DMT.....	38
17. All Activation Curves.....	48

## ABSTRACT

Cloud condensation nuclei (CCN) serve as the nucleation sites for the condensation of water vapor in Earth's atmosphere and are important for their effect on climate and weather. The influence of CCN on cloud radiative properties (aerosol indirect effect) is the most uncertain of quantified radiative forcing changes that have occurred since pre-industrial times. CCN influence the weather because intrinsic and extrinsic aerosol properties affect cloud formation and precipitation development. To quantify these effects, it is necessary to accurately measure CCN, which requires accurate calibrations using a consistent methodology. Furthermore, the calibration uncertainties are required to compare measurements from different field projects. CCN uncertainties also aid the integration of CCN measurements with atmospheric models. The commercially available Droplet Measurement Technologies (DMT) CCN Counter is used by many research groups, so it is important to quantify its calibration uncertainty.

Uncertainties in the calibration of the DMT CCN counter exist in the flow rate and supersaturation values. The concentration depends on the accuracy of the flow rate calibration, which does not have a large (4.3 %) uncertainty. The supersaturation depends on chamber pressure, temperature, and flow rate. The supersaturation calibration is a complex process since the chamber's supersaturation must be inferred from a temperature difference measurement. Additionally, calibration errors can result from the Köhler theory assumptions, fitting methods utilized, the influence of multiply-charged particles, and calibration points used. In order to determine the calibration uncertainties and the pressure dependence of the supersaturation

calibration, three calibrations are done at each pressure level: 700, 840, and 980 hPa. Typically 700 hPa is the pressure used for aircraft measurements in the boundary layer, 840 hPa is the calibration pressure at DMT in Boulder, CO, and 980 hPa is the average surface pressure at Grand Forks, ND.

The supersaturation calibration uncertainty is 2.3, 3.1, and 4.4 % for calibrations done at 700, 840, and 980 hPa respectively. The supersaturation calibration change with pressure is on average 0.047 % supersaturation per 100 hPa. The supersaturation calibrations done at UND are 42-45 % lower than supersaturation calibrations done at DMT approximately 1 year previously. Performance checks confirmed that all major leaks developed during shipping were fixed before conducting the supersaturation calibrations. Multiply-charged particles passing through the Electrostatic Classifier may have influenced DMT's activation curves, which is likely part of the supersaturation calibration difference. Furthermore, the fitting method used to calculate the activation size and the limited calibration points are likely significant sources of error in DMT's supersaturation calibration.

While the DMT CCN counter's calibration uncertainties are relatively small, and the pressure dependence is easily accounted for, the calibration methodology used by different groups can be very important. The insights gained from the careful calibration of the DMT CCN counter indicate that calibration of scientific instruments using complex methodology is not trivial.



## CHAPTER I

### INTRODUCTION

Atmospheric aerosols have an important effect on global climate and weather. Aerosols can influence the climate by scattering and absorbing incoming shortwave radiation and absorbing outgoing longwave radiation. Aerosol effects on the planetary radiation budget are classified as direct and indirect effects. The effect that aerosols have simply due to their radiative properties is known as the aerosol direct effect. Aerosols such as black carbon can absorb solar radiation, leading to a warming effect. However, the aerosol direct effect primarily acts to cool the atmosphere overall by reducing the energy reaching the surface. The aerosol indirect effect accounts for how aerosols affect the global radiation budget through their influence on cloud properties. The aerosol indirect effect is particularly important because clouds are the most important contribution to global reflection of incoming solar radiation (Twomey, 1974). Not all aerosols contribute to the aerosol indirect effect, rather primarily those with an affinity for water vapor, known as cloud condensation nuclei (CCN). Cloud properties are related to CCN concentration, with an increase in CCN resulting in increased cloud droplet concentration, decreased cloud droplet diameter, and increased cloud reflectance. Additionally, there is evidence to suggest that increased CCN concentrations can lead to longer cloud lifetimes and affect global radiative properties (Lindsey and Fromm, 2008). While research has established links between CCN and cloud properties, there is great uncertainty in quantifying the effects of CCN on clouds because of the complexity of aerosol-cloud interactions and the strong

impact clouds have on the planetary radiation budget (Forster et al. 2007). As reported by the Intergovernmental Panel on Climate Change, the indirect effect of aerosols on cloud albedo, and thus climate, is the most uncertain of quantified radiative forcing changes that have occurred since pre-industrial times (IPCC AR5, 2014). Because of this uncertainty, there is a great desire among the research community to better understand the aerosol indirect effect for improved climate modeling. As Pierce and Adams (2009) explain, the foundation of the uncertainty in the aerosol indirect effect stems from the uncertainty in the number of CCN, which is a result of uncertainty in aerosol nucleation, emission, and growth rates. This means that current aerosol measurements are not adequate in terms of amount and accuracy. Lee et al. (2013) states that some of the highest uncertainty in global model simulations of CCN is related to CCN properties, such as CCN size and chemical composition. CCN properties are uncertain in part because there are very few CCN measurement sites worldwide, forcing researchers to interpolate and assume CCN properties over vast unmeasured areas. Therefore, one way to improve the accuracy of aerosol cloud interaction parameterizations is to expand the worldwide CCN dataset (Lance et al., 2009; Roberts et al., 2010). Another factor influencing the uncertainty in CCN properties is that CCN measurement uncertainty is not fully understood, making the implementation of aerosol properties into models uncertain as well (Gunthe et al., 2009; Rose et al., 2008). Due to the low density of CCN measurements, most modeling studies relate cloud optical thickness, cloud effective radius, or cloud droplet number concentration to aerosol loading. Aerosol loading is expressed by aerosol optical depth or aerosol index and used as a proxy for CCN concentration (Saponaro et al. 2017). While using proxies for CCN is useful for understanding how changes in CCN concentration impact the aerosol indirect effect, proxies are limited in their ability to understand CCN properties or aerosol-cloud processes. One of the

ways that the uncertainty in aerosol emissions can be reduced is by quantifying the uncertainty of aerosol measurements. In particular, CCN measurement uncertainty is necessary for more accurate modeling and therefore a better understanding of the aerosol indirect effect.

Through the aerosol indirect effect, CCN can influence the atmosphere with their ability to condense water vapor and grow into droplets through heterogeneous nucleation. Heterogeneous nucleation is the process by which aerosols provide the nucleation site that lowers the energy necessary for phase transition from water vapor to liquid droplets. When the air is saturated (vapor pressure and saturation vapor pressure are equal) an equilibrium is established between condensation and evaporation. However, adding water vapor to the system does not necessarily create droplets because of the free energy barrier to phase transition. Because of this barrier, the saturation ratio (vapor pressure to saturation vapor pressure ratio) would be several hundred percent for condensation to occur in the atmosphere without the presence of nuclei. The reason that water vapor condenses at a saturation ratio near equilibrium in the atmosphere is because CCN are present and have an affinity for water vapor, which significantly reduces the energy required for a phase change.

Supersaturation occurs when there is more water vapor in the air than required for thermodynamic equilibrium. Supersaturated conditions exist in the atmosphere mainly due to rising motions where an air parcel cools, which lowers the saturation vapor pressure causing the water vapor content to exceed that of saturation over a plane water surface. While CCN aid in the formation of droplets, their properties determine how much energy is required in the form of supersaturation to get over the phase transition energy barrier and subsequent droplet growth characteristics. CCN properties such as chemical composition and size are included in Köhler theory, which is used to calculate the supersaturation (“critical supersaturation”) at which a

particular CCN activates. Based on the chemical properties of CCN, information about droplet growth can be calculated. The basic Köhler equation for saturation ratio,  $S$ , over an aqueous solution droplet can be defined as:

$$S = a_w \exp\left(\frac{4 \sigma_{s/a} M_w}{RT \rho_w D}\right), \quad (1)$$

where  $a_w$  is the activity of water in solution,  $\rho_w$  is the density of water,  $M_w$  is the molecular weight of water,  $\sigma_{s/a}$  is the surface tension of the solution/air interface,  $R$  is the universal gas constant,  $T$  is temperature, and  $D$  is the diameter of the droplet (Petters and Kreidenweis, 2007). There are several variations of the basic Köhler model for hygroscopic growth, where parameters are approximated, or assumed constant. One such Köhler theory variation was developed by Petters and Kreidenweis (2007) which uses a single hygroscopicity parameter,  $\kappa$ , to encompass the effects of aerosol chemical composition on water activity. The derivation done by Petters and Kreidenweis (2007) yields the equation:

$$S(D) = \frac{D^3 - D_d^3}{D^3 - D_d^3 (1 - \kappa)} \exp\left(\frac{4 \sigma_{s/a} M_w}{RT \rho_w D}\right), \quad (2)$$

where  $D_d$  is dry particle diameter and  $\kappa$  is the hygroscopicity parameter. Equation (2) applies to any relative humidity and aerosol hygroscopicity. For  $\kappa > 0.2$ ,  $\kappa$  can be calculated from the approximate expression:

$$\kappa = \frac{4A^3}{27 D_d^3 \ln^2(S_c)}, \quad (3)$$

where  $S_c$  is the critical supersaturation corresponding to the dry diameter, and  $A$  is defined as:

$$A = \frac{4 \sigma_{s/a} M_w}{RT \rho_w}, \quad (4)$$

$\kappa$  can be between 0 and  $\sim 1.4$  for atmospherically relevant aerosols. Lower  $\kappa$  values

indicate less hygroscopic behavior, while higher kappa values indicate a more hygroscopic particle.

The role of CCN in the aerosol direct and indirect effects is understood through what is known about CCN activation, droplet growth, and supersaturation. However, accurate measurements of CCN are needed to lower uncertainty in our understanding of the aerosol direct and indirect effects. Researchers face several challenges when taking CCN measurements because of the nature of CCN. The first challenge is that aerosols must be grown to sizes detectable by an optical particle counter since CCN diameters are much smaller than the wavelength of visible light. Activating and growing CCN to detectable sizes is done by establishing supersaturated conditions inside the growth chamber of a CCN counter. Supersaturated conditions are established by saturating the walls of the chamber with respect to water vapor and applying a strong temperature gradient across the chamber. By adjusting the temperature gradient of the chamber the supersaturation is adjusted. Once a supersaturation is established inside a CCN counter, the CCN will activate and grow. Some CCN counters in past decades have used static thermal gradient methods, which involve injecting a sample into the droplet growth chamber, growing the CCN, and counting the grown droplets (Hudson, 1993). An alternate method, which utilizes continuous flow through the droplet growth chamber, is currently the most widely used method for measuring CCN and was first developed by Sinnarwalla and Alofs (1973) and Hudson and Squires (1973; 1976). The continuous flow method is advantageous because it allows for more samples to be processed more quickly as an optical particle counter counts grown droplets as they exit the droplet growth chamber.

Another measurement challenge is that the concentration of CCN is a function of supersaturation. Knowledge of the supersaturation spectra is desirable due to the high variability

of CCN concentration over different supersaturations (Alofs and Liu, 1981), and because cloud supersaturation has been observed to vary greatly. In most CCN counters, observations represent CCN concentration as a function of water vapor supersaturation. Since the critical supersaturation is a function of particle size when the chemical composition is known, it is possible to know the lower limit of CCN size at a single supersaturation. Furthermore, changing the supersaturation in the instrument gives the ability to determine CCN concentration at each supersaturation, producing a CCN supersaturation spectrum. In the quest for an instantaneous CCN spectrometer, some have argued that particle size can be backed out from the measured droplet distribution based on the assumption that particles with the same critical supersaturation will grow the same way in identical supersaturation fields (Hudson, 1989), but this has since been proven not to be the case (Roberts and Nenes, 2005). Without a viable instantaneous CCN spectrometer, the time it takes to develop a CCN spectrum is typically on the order of minutes because the instrument supersaturation must be changed for each measurement. When the time constraints and spatial variability of CCN are taken into account, researchers are limited to stationary platforms to develop the most accurate CCN spectra. The methods used to take CCN spectra rely on knowing the instrument supersaturation; however, to infer CCN size the chemical composition of sampled CCN must be known. Limitations in the ability to measure chemical composition in real-time make doing so nearly impossible, so CCN chemical composition has to be assumed. One way of representing the chemical composition of CCN is to hold the supersaturation constant in the CCN counter while size selecting aerosols, and calculate the kappa value using Eq. 3. The kappa value provides a description of the hygroscopicity of the sample aerosols as a whole. Since the methods to determine CCN size rely on inferences made using Köhler theory based on the water vapor supersaturation inside the instrument, CCN size

calculations will only be as accurate as the supersaturation calibration of the instrument. But, determining the supersaturation in the CCN counter is also done indirectly. When aerosol size and chemical composition are fixed, an accurate supersaturation can be determined using Köhler theory. The process of inferring aerosol properties is what leads to high uncertainties in CCN measurements, so if the supersaturation calibration is more accurate, the inferences made about aerosol properties will be less uncertain.

A CCN counter that uses the continuous flow method for measuring CCN concentration is the commercially available Droplet Measurement Technologies (DMT) CCN Counter (Roberts and Nenes, 2005). The DMT CCN counter can develop a CCN spectrum as quickly as 12 minutes by changing the chamber's temperature gradient. However, recent research has developed a method whereby the instrument sample flow rate is continuously changed with a special pump attachment, which continuously changes the supersaturation. This permits a supersaturation spectrum to be determined in less than a minute (Moore and Nenes, 2009). Due to its design and availability, the DMT CCN counter is the most widely used counter in the world with over two hundred instruments in use. Because of the DMT CCN counter's widespread use, researchers can effectively compare measurements across different field projects. While using the same instrument type aids in the comparability of measurements, other factors can affect measurement comparability, including the calibration of the instruments. CCN counter calibrations are not trivial and calibration methodology may lead to differences between instruments from the same manufacturer. Thus, it is important to quantify the uncertainties that can be passed on to measurements through an instrument's calibration. Rose et al. (2008) used a wide range of instrument operating conditions (temperature, pressure, and flow rate) and Köhler model calculations to determine the uncertainty of CCN measurements for the DMT CCN

counter. They were able to find relative deviations in effective supersaturation inside the instrument, dependence of supersaturation on pressure, temperature, and flow rate, and overall relative deviation in the supersaturation calibration. Roberts et al. (2010) were able to expand on the work done by Rose et al. (2008) by experimentally deriving an expression describing the instrument's supersaturation related to temperature and pressure.

Since the DMT CCN counter is commonly used in atmospheric research on aircraft, it is important to verify the supersaturation pressure dependence that has been found in addition to overall uncertainty. On an aircraft it is not as easy to maintain the flow rate and sample temperature as it is on the ground and maintaining constant chamber pressure is very difficult. Due to the relatively fast changes in altitude an aircraft can undergo during sampling, a constant pressure inlet must be used, which is typically set to a lower, constant value (~700 hPa for measurements in the boundary layer). Since the pressure must be lowered for stable CCN measurements on an aircraft, the instrument's sampling pressure is different from the pressure where the supersaturation is typically calibrated. Therefore, understanding the supersaturation dependence on pressure has implications for aircraft CCN measurements. This research examines whether a pressure correction should be performed on the instrument's calibration, or if the calibration uncertainties at lower pressures warrant calibrating at aircraft sampling conditions. In order to understand how the calibration uncertainties affect the CCN counter's measurements, this research will go further by applying the calibration uncertainties to measurements.



## CHAPTER II

### METHODOLOGY

The DMT CCN counter depends on three main calibrations for accurate concentration measurements. Each calibration affects the instrument's measurements differently, so understanding individual calibration uncertainties is necessary for an overall understanding of measurement uncertainty. The necessary calibrations include the pressure calibration, flow rate calibrations, and the supersaturation calibration. Due to the complexity of the supersaturation calibration there are certain quality control measures that should be observed when doing the supersaturation calibration. Additionally, since some calibrations are done at lower than ambient pressure there are special considerations that need to be addressed prior to calibration.

The pressure calibration's accuracy is essential since modeling and experimentation indicate that the instrument's supersaturation strongly depends on pressure (Roberts and Nenes, 2005; Rose et al., 2008). Pressure calibration is straightforward using a commercially available calibration standard (e.g. Mensor Model DPG 2300) to determine the relationship between the instrument's pressure transducer voltage and sample pressure. At least five points are measured over the range of 100-1000 hPa and are fitted linearly with the fit equation coefficients being used as the pressure calibration coefficients.

The sheath and sample flows must be calibrated since their ratio determines how confined the aerosols are to the center of the growth chamber. Since the supersaturation is constant along the center of the growth chamber, accurately confining aerosols to the centerline with an accurate

flow ratio is important (Roberts and Nenes, 2005). The sample flow calibration is particularly important because the sample flow rate determines the volume of air in which droplets are counted by the optical particle counter. Each flow rate is calibrated using a Gilian Gilibrator bubble flow meter standard. Ten samples are taken at five valve voltage settings between 0.020-0.075 L min<sup>-1</sup> for the sample flow and 0.200-0.750 L min<sup>-1</sup> for the sheath flow. Ten-sample averages of measured flows are related to instrument voltage through a linear fit. The fit equation coefficients are used as the calibration coefficients for both the sample and sheath flows (Cloud Condensation Nuclei Operator Manual Revision F, 2004 p. 29).

The supersaturation calibration is the most involved of the three calibrations important in determining the CCN counter's calibration uncertainty. This calibration requires a complex lab setup (Figure 3), which includes an air compressor pushing filtered air at 30 psi through a Constant Output Atomizer (TSI Model 3076) filled with 0.05 g/L ammonium sulfate in solution with ultra-pure water. Downstream of the Constant Output Atomizer, aerosols are dried using a desiccant dryer and diluted with filtered air in a mixing box (stainless steel, ~1.95 L). Measurements of the sample air after dilution indicate the sample air has a relative humidity of no more than 15 %, ensuring no condensation will occur on the sample aerosols before they are counted. Precision needle valves on the filter and sample lines to the mixing box are used to regulate the aerosol concentration that enters the Differential Mobility Analyzer (DMA; TSI model 3080 Electrostatic Classifier). For calibrations performed at lower than ambient pressure, a DMT Constant Pressure Inlet (CPI) is installed inline upstream of the DMA to regulate pressure. At the DMA inlet, an impactor (nozzle diameter of 0.071 cm) is used to remove large aerosols (cut size of ~650 nm under 298.15 K temperature and 980 hPa pressure conditions). A neutralizer installed in the DMA is used to normalize and narrow the charge distribution of the

ammonium sulfate aerosols. The voltage applied to the DMA's central rod selects the size of aerosols based on their electrical mobility. A Condensation Particle Counter (CPC, TSI model 3772) and a DMT CCN counter sample the aerosols from the DMA exit. The CPC counts all aerosols larger than 10 nm in diameter, while the CCN counter measures aerosols that activate as droplets.

Since the generated peak aerosol diameter depends on the concentration of ammonium sulfate in solution, it is necessary to measure the size distribution using varying amounts of ammonium sulfate in solution to determine the correct amount to use. The Constant Output Atomizer manual shows how solute concentration affects peak diameter in Fig. 1.

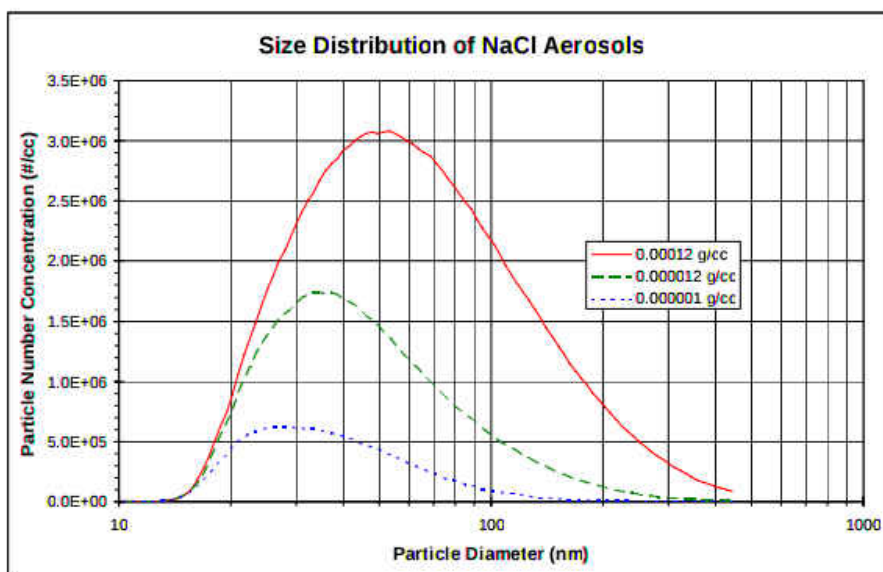


**Figure 1:** Size distributions for different NaCl solutions used in the Constant Output Atomizer (TSI Model 3076). The figure is reproduced from the Model 3076 Constant Output Atomizer Instruction Manual, Revision J, page 36.

The size distribution for the solution that meets the requirements of this research, measured using a Scanning Mobility Particle Sizer (SMPS model 3080-3081L) scan, is shown in Fig. 2.

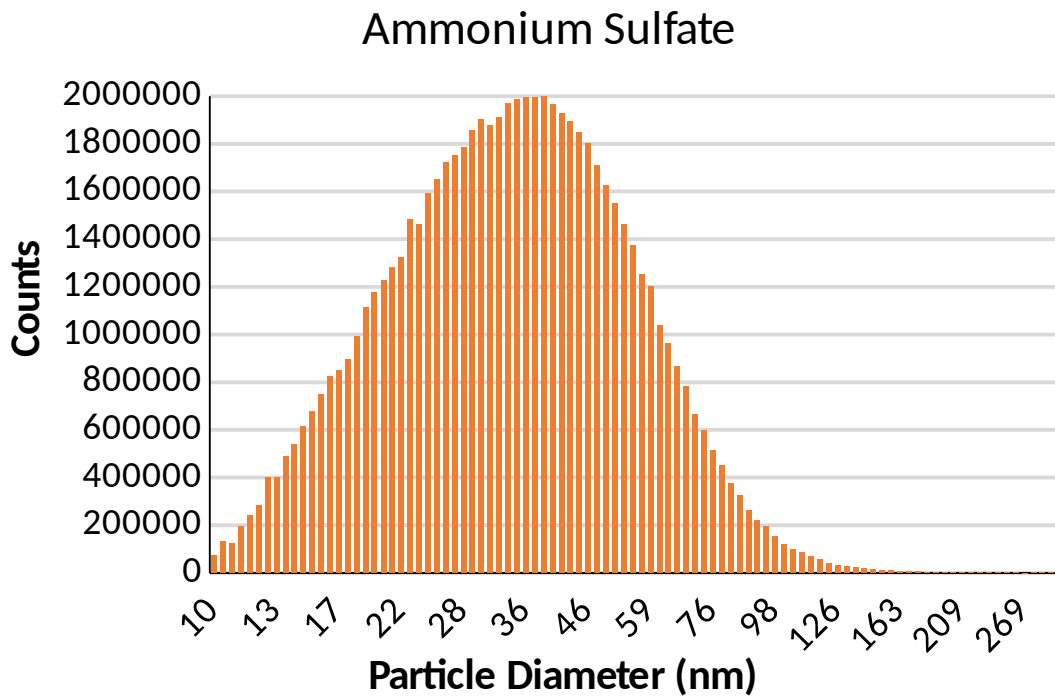


**Figure 2:** Scanning Mobility Particle Sizer (SMPS model 3080-3081L) scan of ammonium sulfate particles generated with a Constant Output Atomizer (TSI Model 3076) on October 18th, 2016. The Constant Output Atomizer uses 30 psi compressed air and an ammonium sulfate solution of 5.0 mg/L.

If the peak in the generated particle size distribution is larger than the particle sizes being selected for the supersaturation calibration there is a risk for multiply charged aerosols influencing the data because chances for double charging increase with increasing size (Wiedensohler, 1988). Furthermore, if concentrations are also higher at larger sizes due to a peak diameter that is too large, the chances for double charging are increased even more. Therefore, it is important to have a generated aerosol size distribution that peaks at the lowest size possible while still maintaining counts of at least  $150 \text{ # cm}^{-3}$  at the highest selected size. Poisson counting statistics indicate that at a concentration of  $150 \text{ # cm}^{-3}$  the relative counting error is less than 10 % (Horvath et al., 1990). The size distribution peak aerosol diameter of generated aerosols can be moved toward lower sizes by diluting the concentration of solute used to generate aerosols

(Model 3076 TSI Constant Output Atomizer User Manual Revision J, 2005). However, if the size distribution peak is too low then concentrations at larger selected aerosol sizes may be too low as the size distribution tails off. Hence, a balance must be achieved in order to minimize double charging while also maintaining high enough aerosol concentrations at large sizes. Since 0.05 g/L solution generates a peak aerosol diameter lower than the smallest activation size (38.5 nm) and a concentration of at least  $150 \text{ \# cm}^{-3}$  at the highest selected size, this solution is used for the calibrations in this research.

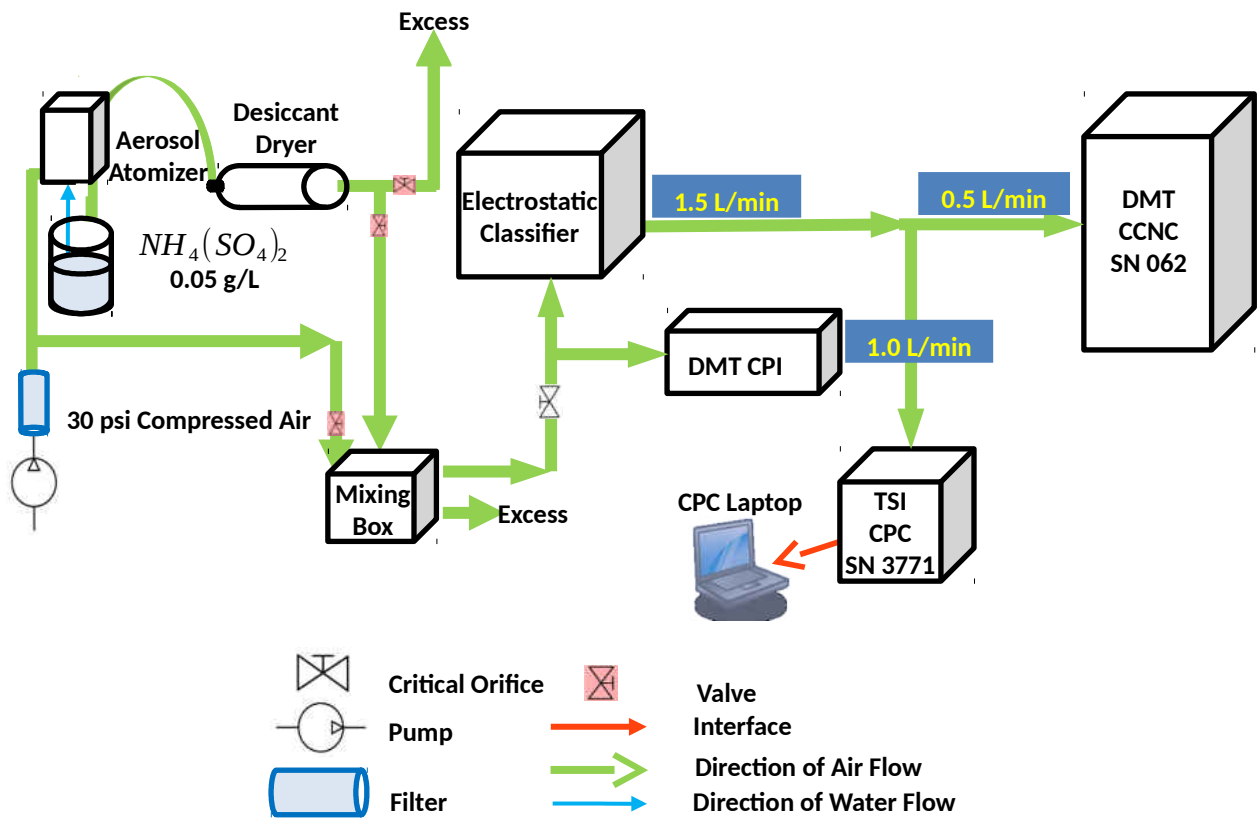


**Figure 3:** Laboratory setup for supersaturation calibrations at prescribed pressures. Boxes show each instrument in the system along with its abbreviated name. Flows associated with each instrument are shown in blue boxes, while arrows denote the direction of flow.

## Instrument Descriptions

With a calibration process that involves the use of several instruments, it is especially important to understand the theory of operation for each component to ensure good data. The TSI Model 3076 Constant Output Atomizer generates particles by forcing compressed air (30 psi) through an orifice to form a high-velocity jet. Liquid is drawn into the jet through a vertical passage and atomized. Large droplets impact on a wall opposite the jet and excess liquid is drained back to the solution bottle, while fine spray leaves the atomizer block through an opening at the top. The fine spray consists of ammonium sulfate solution aerosols (Model 3076 Constant Output Atomizer Instruction Manual Revision J, 2005). Since the supersaturation calibration requires activation of dry aerosols, the solution aerosols are passed through a silica gel diffusion dryer to evaporate all water. In a diffusion dryer, aerosols pass through an inner tube made of wire screen. Silica beads surround the inner tube completely, absorbing water vapor and thus maintaining a dry environment (relative humidity <15%) throughout the aerosol tube. The water in each solution aerosol is therefore evaporated leaving behind a solid particle.

The DMA size selects aerosols based on the direct relationship between electrical mobility and aerosol diameter with singly charged aerosols. After being generated and dried, the aerosols have a range of electrostatic charges and must be neutralized before size selection can occur in the DMA. Without neutralization a wide charge distribution leads to a significantly increased number of large particles being selected unintentionally. Upon entering the DMA, aerosols pass through a Kr-85 neutralizer that exposes them to high concentrations of bipolar ions. Frequent collisions between the aerosols and ions create a state of charge equilibrium, in which the aerosols carry a known bipolar charge distribution consisting primarily of -1, 0, and +1 charges.

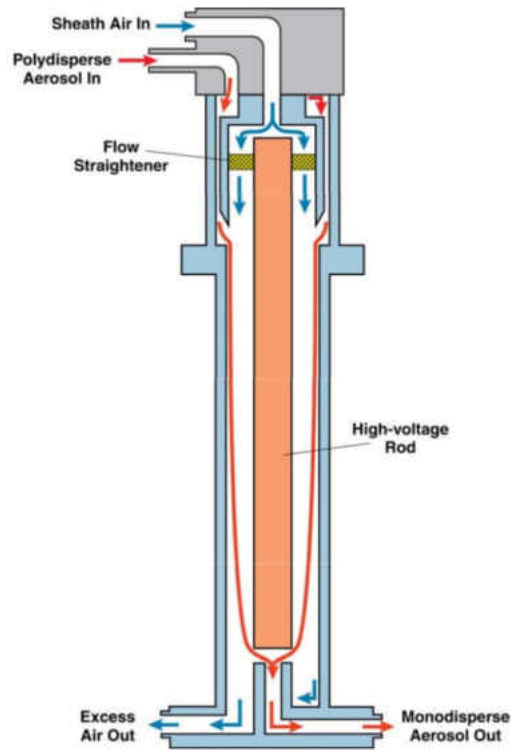


**Figure 4:** Flow diagram of the main portion of the DMA where size selection occurs. Arrows denote direction of flow. The figure is reproduced from the Series 3080 Electrostatic Classifiers Operation and Service Manual Revision G, p. 53.

The main portion of the DMA consists of two concentric cylinders as shown in Figure 4. The polydisperse aerosols and sheath air are introduced at the top of the classifier and flow down through the space between cylinders with the polydisperse flow surrounding the sheath flow. The inner cylinder, or collector rod, is maintained at a controlled negative voltage, while the outer cylinder is grounded creating an electric field between the two cylinders. The electric field causes positively charged aerosols to be attracted through the sheath air to the negatively charged collector rod. Aerosols within a narrow range of electrical mobility exit through a slit at the bottom of the collector rod with the monodisperse air flow. Since multiply charged aerosols can have the same electrical mobility as smaller singly charged aerosols, neutralization removes most multiply charged aerosols before classification reducing classification error. The remaining

aerosols are removed as the rest of the flow recirculates through filters in the DMA to be used again as sheath flow (Series 3080 Electrostatic Classifiers Operation and Service Manual Revision G, 2006).

Once classified, total aerosol concentration is determined with the CPC. The TSI CPC 3772 is a continuous flow, diffusional, alcohol-based, thermal-cooling condensation nuclei counter that can detect aerosols as small as 10 nm in diameter efficiently. The instrument counts with an optical particle counter by measuring the scattered light off of grown droplets. As each droplet scatters light, it is counted by a low-noise photodiode detector. The counted aerosols are attributed to the sample volume passed through the instrument giving an aerosol concentration measurement. To create a supersaturation, the CPC first saturates the sample with butanol by passing the sample through a saturator wick which is kept wet with butanol as the instrument pulls from a reservoir as needed. If the reservoir is empty the CPC automatically pulls more butanol into the reservoir from an outside butanol bottle if it is connected (Condensation Particle Counter Operator Manual Revision C, 2007). The saturated sample then passes through the condenser where the temperature is much lower than the sample temperature creating a supersaturation with respect to butanol of several hundred percent. The temperature difference between the saturation chamber and condenser chamber is set so that all particles larger than 10 nm grow condense butanol and grow rapidly to sizes detectable by the optical particle counter.

The monodisperse aerosol stream is also sampled by the DMT CCN counter. The DMT CCN counter has a vertical droplet growth chamber in which a supersaturation is generated along the centerline to grow droplets. Sample flow is introduced into the center of the chamber at the top while sheath flow is humidified and introduced along the walls. The sheath to sample flow ratio is kept around 10:1 and determines how confined the sample is to the centerline. The inner



walls of the chamber are kept wet using a porous alumina bisque liner and temperatures are controlled at the top, middle, and bottom of the chamber. Based on the principle that water vapor diffuses more quickly in air than heat, the instrument can generate a supersaturation inside the droplet growth chamber (Roberts and Nenes, 2005). As water vapor and heat diffuse toward the center of the chamber, there is more water vapor available than there would be in thermodynamic equilibrium, thus creating a supersaturation (Cloud Condensation Nuclei Counter Operator Manual Revision F, 2004). The centerline supersaturation at the bottom of the droplet growth chamber depends on the temperature difference between the top and bottom of the chamber, the flow rate, and the absolute pressure in the chamber (Roberts and Nenes, 2005). Once droplets activate in the chamber, they rapidly grow to detectable sizes (0.75 - 10  $\mu\text{m}$ ). An optical particle counter at the exit of the chamber uses standard light scattering techniques to count particles and sizes them into 20 bins.

### Calibration Methodology

While temperature gradient ( $\Delta T$ ), pressure, and flow rate influence supersaturation, only  $\Delta T$  is varied when doing the supersaturation calibration. For each  $\Delta T$  in the supersaturation calibration,  $\Delta T$  is kept constant while the particle size is varied using the DMA. At the start of sampling for each size, the system is allowed to flush and come into equilibrium before acquiring data. After a two minute equilibration, data are acquired in the CPC and DMT CCN counter at a frequency of 1 Hz for one minute. The data are averaged and the CCN to CPC (CCN/CPC) ratio is calculated from the one minute averages. The smallest size for each  $\Delta T$  should give a CCN/CPC ratio of zero, otherwise lower sizes are sampled until a zero ratio is achieved to form a baseline of no activation. From the zero ratio, sizes are increased by 5 nm until the CCN/CPC ratio levels off. Following data acquisition, data are merged and processed (see Appendix A)

using the Airborne Data Processing and Analysis (ADPAA) software package (Delene, 2011). Processing generates activation curve plots and data files for each  $\Delta T$ . From these activation curves and data files, the activation sizes are determined based on the size at which the activated ratio passes half the maximum value of the activated ratio (Rose et al. 2008). The process of determining activation size is described in more detail in the data section. The calculated activation size is related to a critical supersaturation percentage using kappa-Köhler theory as defined by Petters and Kreidenweis (2007). The size selecting process is repeated for five  $\Delta T$ 's. Three supersaturation calibrations are done at each of three pressure levels: 700 hPa, 840 hPa, and 980 hPa. These pressures are used because 700 hPa is the typical operating pressure for aircraft observations with the DMT CCN counter, 840 hPa is the pressure at DMT in Boulder, CO where the CCN counters are calibrated by DMT, and 980 hPa is the average ambient pressure in Grand Forks, ND over the course of calibrations. The standard deviation for each series of three calibration points is calculated as a measure of the relative uncertainty of each point on the calibration line. The percent error of the calibration points with respect to each calibration line is calculated to give the overall uncertainty of the calibrations. A supersaturation calibration equation is developed for each calibration by relating  $\Delta T$  to calculated supersaturation percentage and applying a linear fit to the data. The coefficients of the supersaturation calibration fit equation are used as the calibration coefficients in the instrument.

### Quality Control

When calibrating at a reduced pressure, it is especially important to ensure the system is leak-tight so laboratory air does not contaminate the generated aerosol sample. In order to leak check the system, the filtered air inlet and exhaust at the mixing box are plugged. The CPC is removed and its line is capped since applying a vacuum to the CPC affects its operation. CPC

pressure effects are covered extensively in the Special Considerations section. A hand-held vacuum pump is attached to the sample inlet of the mixing box and used to pump the system down to 10 in Hg of pressure (~650 hPa). If the system pressure rises by 0.5 in Hg in less than 5 minutes an unacceptable leak is present in the system. Finding the leak requires removing one section of the system at a time and leak testing the remaining system as previously described until the leak significantly improves. The section or sections responsible for the leak are repaired or replaced until the whole system can meet leak-tight standards. While most of the calibration system consists of Swagelok materials, the DMT CCN counter uses some non-Swagelok fittings. Even though Swagelok materials can leak, the components that leak most often are the non-Swagelok plastic fittings inside the DMT CCN counter. Furthermore, it has been our experience that every time the DMT CCN counter is shipped it arrives with leaks present in the plastic fittings. When the system passes a leak check data can be acquired, but other quality control measures are necessary to maintain accuracy.

Since the silica gel in the diffusion drier can absorb only a finite amount of water vapor, it is necessary to regenerate the silica gel frequently. The silica gel is regenerated when the dark blue beads along the wire tube begin to turn pink, which indicates that the silica gel can no longer absorb water vapor effectively. This must be done after approximately every five hours of operation and is accomplished by microwaving until all beads have returned to their dark blue original color. If the silica beads are not regenerated, aerosols won't thoroughly dry, leading to inaccurate aerosol size selection.

In order to maintain proper flow rate through the system, the impactor at the inlet of the DMA must be cleaned periodically. If aerosols build up on the impactor and it is not cleaned, flow can be obstructed altering the flowrate through the DMA. The DMA manual states that the

impactor must be cleaned every 5-50 hours of operation; for the supersaturation calibration the impactor is cleaned every 10 hours.

### Special Considerations

Special considerations must be made to ensure instruments are operating properly at lower than ambient pressures. The main obstacle to operating under lower pressures is that the CPC is designed to operate under ambient conditions. Therefore, in order to correctly operate the CPC at lower pressures, an understanding of its theory of operation is useful (see Appendix B). When lowering pressure, and operating under low pressure, the operator ensures the wick is saturated by letting the instrument warm up under ambient conditions connected to a butanol source. In order to lower pressure the operator first disconnects the butanol source from the CPC. The pressure is lowered very slowly with filtered air entering the system and the DMT CCN counter off to ensure the CCN counter is not contaminated from potential butanol release. The process of lowering pressure with the DMT CPI pulls flow against the CPC. If the CPC flow drops below that of the DMT CPI butanol is sucked upwards from the reservoir in the CPC. If there is too much butanol in the reservoir or if the operator lowers pressure too quickly, butanol will be sucked upwards and onto the saturator wick. The excess butanol on the saturator wick gets caught in the sample stream and butanol is deposited on the OPC lens. This phenomenon is known as flooding, which distorts the normal light scattering in the OPC giving very inaccurate and erratic counts. If the instrument floods, pressure is immediately raised until CPC counts are able to return back to zero. This procedure is repeated several times until the desired pressure is reached without flooding the CPC. Effectively this procedure will empty the reservoir safely to a level that butanol will not be lofted onto the OPC. However, with the supply bottle disconnected, the saturator wick contains only enough butanol for six hours of operation,

so calibrations at lower pressures are restricted to six hours from the time the CPC is turned on. The procedures outlined above apply for a CPC with a critical orifice installed which maintains flow at  $1.0 \text{ L min}^{-1}$  (normal operation). Alternatively, the critical orifice can be removed and a flow controller can be installed downstream of the CPC and upstream of its pump. While the flow controller is set to  $1.0 \text{ L min}^{-1}$ , pressure can slowly be lowered as outlined previously while the CPC is not connected to a butanol source. Limitations in how quickly pressure can be reduced and operating time still apply when using a flow controller instead of a critical orifice.

After properly reaching the prescribed pressure without flooding the CPC, the DMT CCN counter is turned on. Reduced pressure may also fog up the OPC in the DMT CCN counter. At the OPC in the DMT CCN counter the “1<sup>st</sup> Stage Monitor” displays a voltage corresponding to the amount of obstruction between the laser and the OPC. If this value is above 0.40 V, then there are likely water droplets or other contaminants blocking the OPC leading to inaccurate CCN counts (Cloud Condensation Nuclei Counter Operator Manual Revision F p. 30, 2004). Under normal operating conditions, problems with OPC fogging are not common, but when operating at lower than ambient pressure the OPC may fog up. Solutions for the OPC fogging include waiting for the issue to resolve on its own, increasing flow rate through the DMT CCN counter, or setting the column temperature gradient to zero while increasing the OPC temperature. While the full cause of OPC fogging is not clear, and thus cannot be properly prevented, it is important to ensure measurements are taken at reduced pressure only after the 1<sup>st</sup> Stage Monitor remains below 0.40 V under ambient conditions.

While pressure is controlled by the DMT CPI, the impactor in front of the Electrostatic Classifier also has an effect on pressure. The impactor inlet is a nozzle which lowers the pressure approximately 30 hPa with a flowrate of  $1.5 \text{ L min}^{-1}$ . Thus, when operating at ambient

conditions the impactor must be taken off the inlet to the Electrostatic Classifier to keep the calibration system at truly ambient conditions. Removing the impactor does not affect the performance of the Electrostatic Classifier because of the small aerosol sizes being used in this research.

## CHAPTER III

### DATA

Calibration of the DMT CCN counter involves a series of different calibrations, starting with a pressure calibration. Although the pressure calibration is not expected to change over time, it is important because of the effects that pressure has on the CCN counter's supersaturation. The pressure calibration shows that the pressure transducer voltage is linearly related to the absolute pressure standard (Fig. 5). Over the six year history of the Serial Number 062 CCN counter, the pressure calibration has changed by less than 1 %, thus introducing negligible uncertainty into the instrument's supersaturation. After the pressure calibration, the sheath and sample flow calibrations are conducted (Figs. 6 and 7).

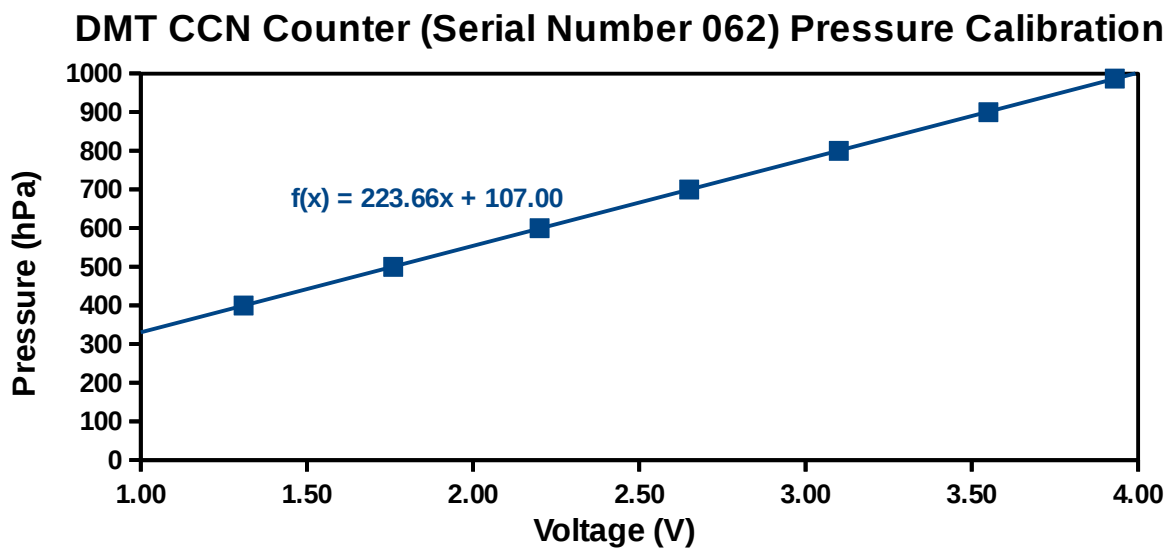


**Figure 5:** Pressure calibration conducted on 18 May 2016 in the University of North Dakota Instrumentation Laboratory (CH423). The Mensor Model DPG 2300 pressure standard is used as the calibration standard. Calibration data points are fitted linearly and the trend line equation coefficients are used as the Droplet Measurement Technologies (DMT) cloud condensation nuclei (CCN) counter pressure calibration coefficients.

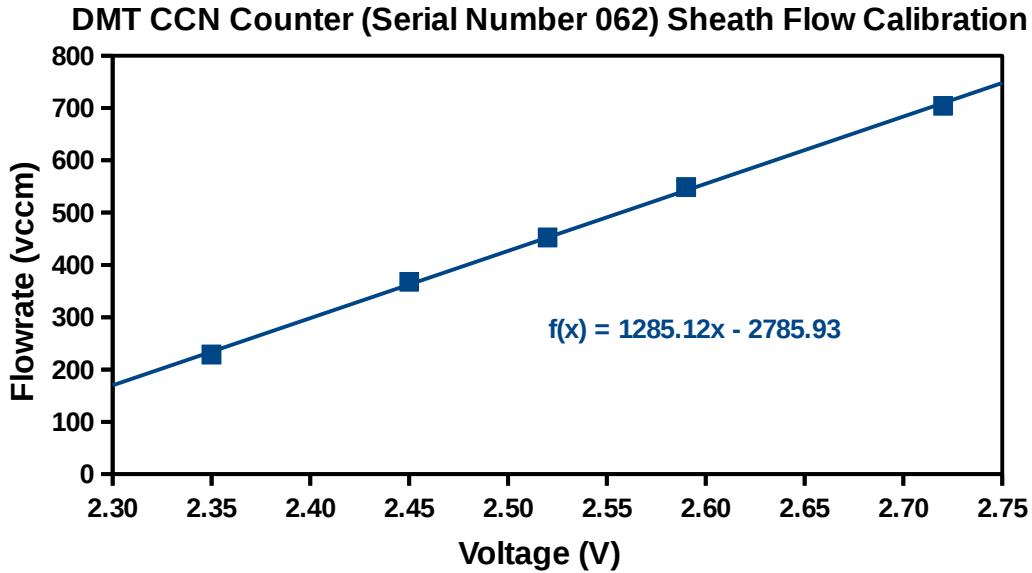


**Figure 6:** Sheath flow calibration conducted on May 18<sup>th</sup>, 2016 in the University of North Dakota Instrumentation Laboratory (CH423). The Gilian Gillibrator bubble flow standard is used as the calibration standard. A linear least squares fit is applied to the calibration data points and the fit equation coefficients are used as the Droplet Measurement Technologies (DMT) cloud condensation nuclei (CCN) counter sheath flow calibration coefficients.

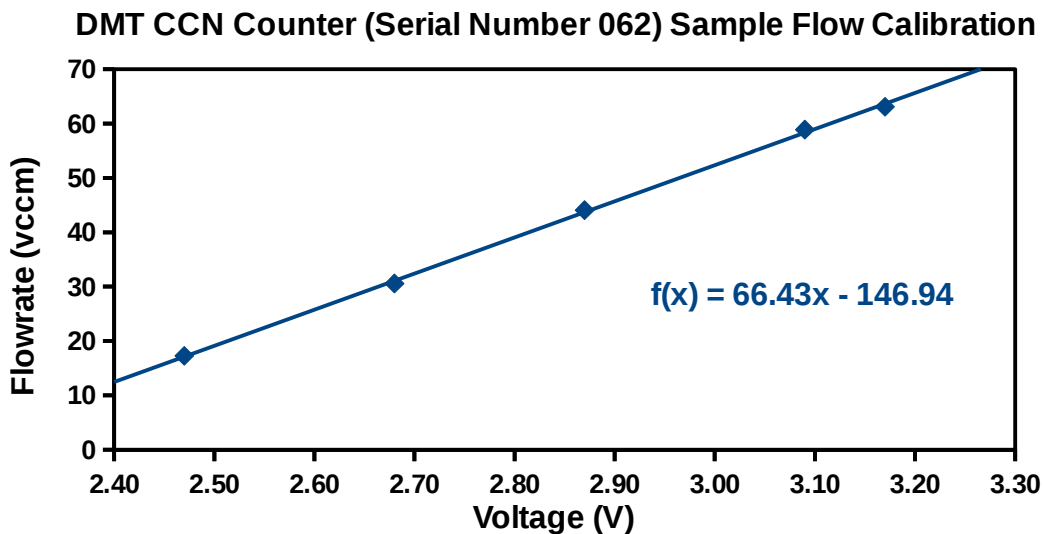


**Figure 7:** Sample flow calibration data taken on May 18<sup>th</sup>, 2016 in the University of North Dakota Instrumentation Laboratory (CH423). The Gilian Gillibrator bubble flow standard is used as the calibration standard. A least squares linear fit is applied to the calibration data points and the fit equation coefficients are used as the Droplet Measurement Technologies (DMT) cloud condensation nuclei (CCN) counter's sample flow calibration coefficients.

After a period of 6 months a performance check is conducted on the sheath flow and sample flow calibrations. With a set point of 0.455 L min<sup>-1</sup>, the ten sample average of the



counter's sheath flow is  $0.443 \text{ L min}^{-1}$ , which represents a 2.5 % error; however, an error of at least 10 % is required for a significant impact on measurements. With a set point of  $0.045 \text{ L min}^{-1}$ , the ten sample average measured sample flow is  $0.047 \text{ L min}^{-1}$  representing a 4.3 % error in sample flow. Since any error in sample flow affects concentration measurements, the sample flow error will be examined more closely in Chapter IV.

The most complex calibration is the supersaturation calibration. One of the important elements of the supersaturation calibration is the creation of activation curves from concentration measurements made by the CCN counter and CPC, which are expressed as the CCN/CPC concentration ratio. Figure 8 shows activation curves that match the activated ratio data well (all activation curves are in Appendix C). An activation curve is generated for each  $\Delta T$  (6, 8, 10, 12, and 14 K) used in the supersaturation calibrations. Each activation curve is fitted with a sigmoidal curve.

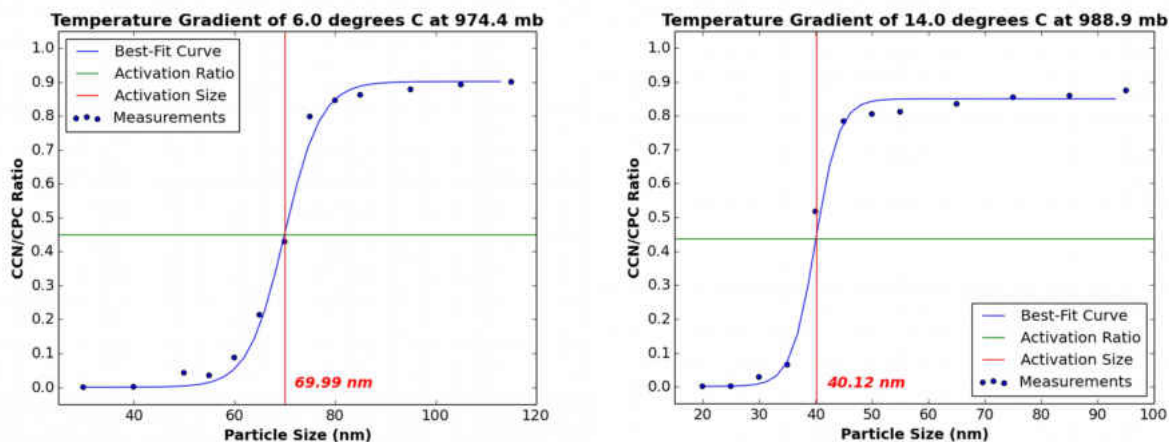


**Figure 8:** Activation curve fits of measured ratio data taken on October 28th, 2016 in the University of North Dakota Instrumentation Laboratory with the instrument operating at ambient pressure ( $\sim 980 \text{ hPa}$ ) and  $\Delta T$  of 6 and 14 degrees Celsius. The data are fitted with a sigmoidal curve using the Python SciPy curve\_fit module. The activation size is represented by the red vertical line, as well as displayed in red italicized text. The activation ratio is represented by the horizontal green line.

The point at which the fit line passes through the activation ratio is defined as the activation size, where activation ratio is defined as half of the maximum ratio of the activation curve. While the ideal value is 0.5, deviations from 0.5 can occur through particle losses and instrument measurement errors. To account for a maximum ratio not equal to 1.0, the ratio data can be adjusted by normalizing so the maximum value is 1.0. Since normalizing is symmetric with regard to the activation ratio, normalization does not affect the value of the activation size (Rose et al., 2007). Plateaus in the CCN/CPC ratio data are apparent (Fig. 8) at particle sizes smaller than the activation sizes. These plateaus exist due to multiply charged particles being selected by the Electrostatic Classifier. The multiply charged particles are larger than the selected size, but because of their higher charge state, have the same electrical mobility as the selected size. Since a neutralizer is used, the fraction of multiply charged particles remains below 5 % throughout all calibrations. Although plateaus of any height can affect the calculated activation size, Rose et al. (2008) shows that a plateau below 10 % has a negligible affect (< 0.5%) on calculating the activation size. In order to minimize the plateau's effect further, the first data point in the activation curve is heavily weighted (99 % certainty) since it is known to be zero with other points weighted equally (0.01 % certainty).

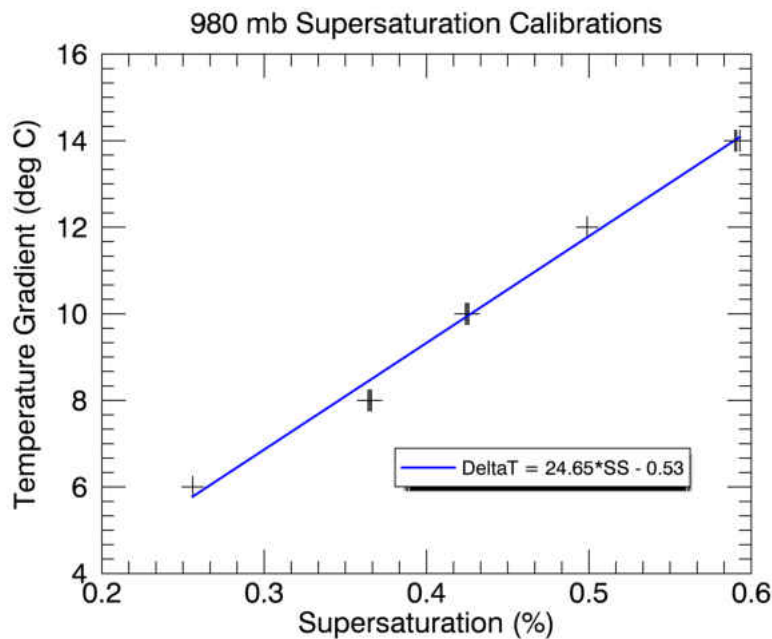


**Figure 9:** Supersaturation calibrations done between October 28<sup>th</sup> and November 5<sup>th</sup>, 2016 in the University of North Dakota Instrumentation Laboratory (ambient pressure of approximately 980 hPa). Three data points are taken at each  $\Delta T$ . A least squares linear fit is used to determine the given supersaturation calibration equation.

The activation size is used to determine the supersaturation for each  $\Delta T$  using kappa-Köhler theory (Petters and Kreidenweis, 2007). A set of five  $\Delta T$ s and corresponding calculated supersaturations are used to determine the instrument's supersaturation calibration (Fig. 9). The supersaturation versus  $\Delta T$  data are fitted linearly to give the supersaturation calibration coefficients for the DMT CCN counter. Three activation curves are obtained at each  $\Delta T$  to enable the relative standard deviation of supersaturation to be calculated, which is used as the uncertainty in calculating supersaturation. Overall, the uncertainty in calculated supersaturation is between 0.1-0.3 %, showing agreement with the similarly small relative deviations of 1% found by Rose et al. (2008). The very low relative deviations in supersaturation at each  $\Delta T$  can be seen in Figs. 9, 10, and 11 as the points at each  $\Delta T$  are nearly on top of each other. The lower relative deviations found in this research are most likely due to the longer averaging interval of at

least 1 minute instead of an interval of 20-30 seconds. The uncertainty in each calibration ranges from 2.3-4.4% increasing with decreasing pressure. This is likely due to the possible non-linearity of the calibration line. The DMT CCN counter operator manual notes that below 0.1% the calibration curve becomes non-linear, however it is possible this non-linearity may have moved over time with physical changes inside the instrument. If the calibration line has a non-linear element at the lower end, and lower pressures mean lower supersaturations in general, then more of the calibration line will be influenced by the non-linear element at lower pressures leading to higher uncertainties.

While uncertainties change with pressure, there are also other notable changes in the supersaturation calibration related to pressure. The calibration line shifts toward lower supersaturations and has a steepening slope at reduced pressures. With decreasing pressure the slope of the calibration line increases by 5.4% per 100 hPa. This effect can be seen in Figs. 10 and 11 showing the 840 hPa and 700 hPa calibrations respectively.

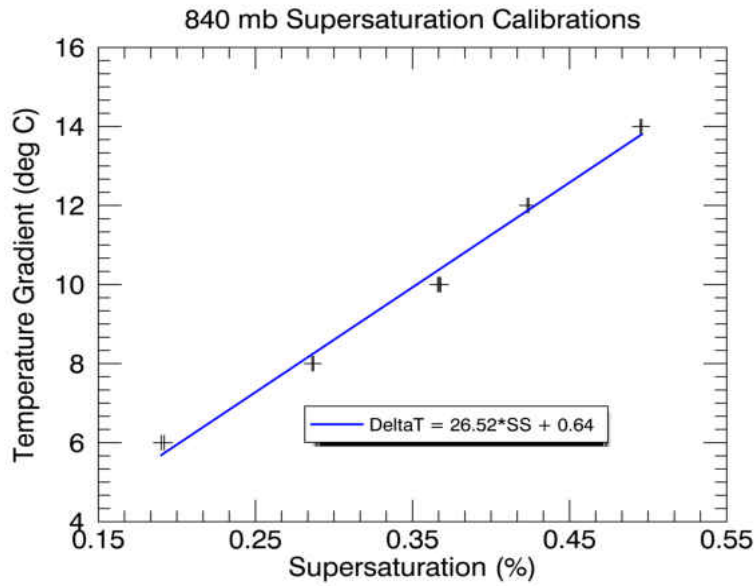


**Figure 10:** Supersaturation calibrations at 840 hPa done between November 17<sup>th</sup>-19<sup>th</sup>, 2016 in the University of North Dakota Instrumentation Laboratory. Three data points are taken at each  $\Delta T$ . A least squares linear fit is used to determine the given supersaturation calibration equation.

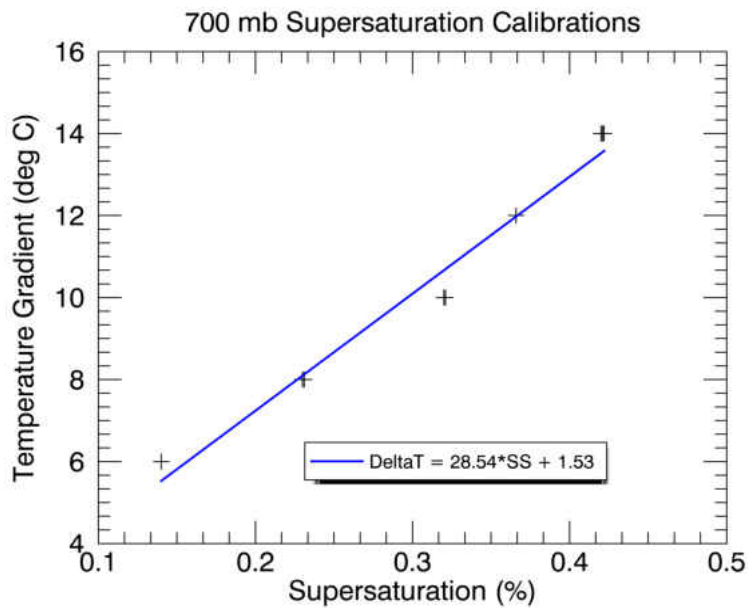


**Figure 11:** Supersaturation calibrations at 700 hPa done between November 8<sup>th</sup>-15<sup>th</sup>, 2016 in the University of North Dakota Instrumentation Laboratory. Three data points are taken at each  $\Delta T$ . A least squares linear fit is used to determine the given supersaturation calibration equation.

As Rose et al. (2008) noted, the shift in the calibration line toward lower supersaturations is not constant, but nearly-linear with changing  $\Delta T$ . In this research, the pressure dependence appears not to be constant with changing  $\Delta T$  due to the changing calibration slope with pressure; however, the effect is small and difficult to discern. On average, the calibration line shifts toward lower supersaturations at a rate of 0.047 % per 100 hPa. Figure 12 gives a more detailed description of how the supersaturation changes with pressure and  $\Delta T$ . Despite the nearly constant pressure dependence with changing  $\Delta T$ , it is possible to quantify the effects  $\Delta T$  has on the supersaturation pressure dependence. Figure 13 shows the pressure dependence of the supersaturation based on the  $\Delta T$ .

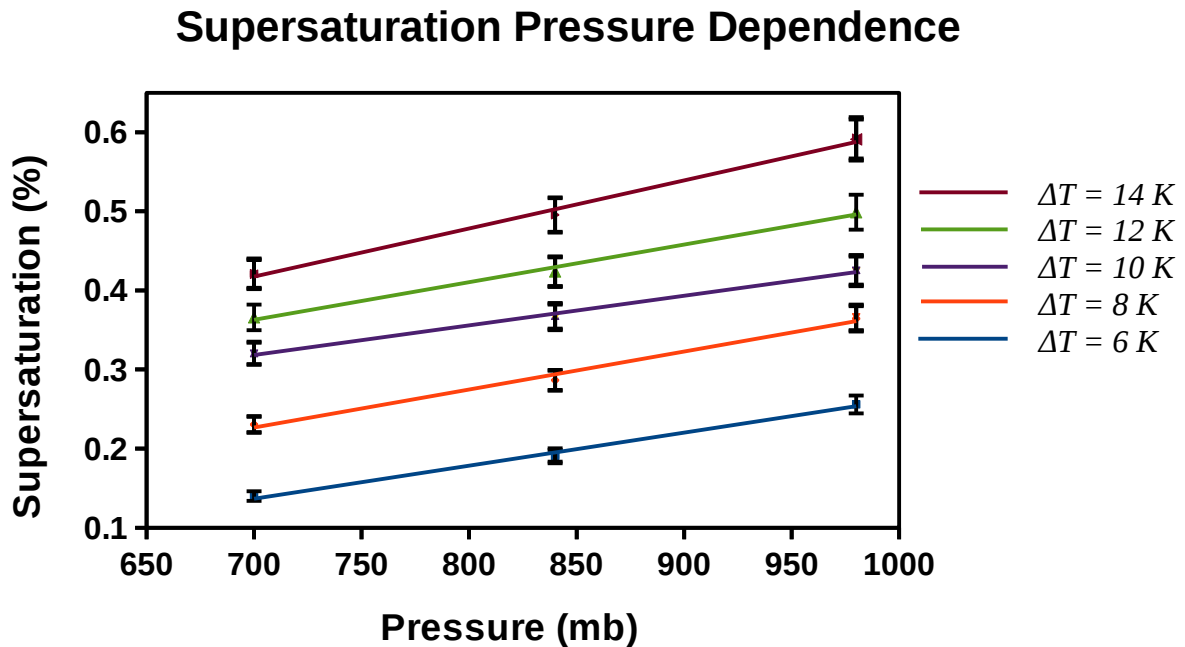


**Figure 12:** Calculated supersaturation is shown at each pressure level where calibrations were performed. Each fit line corresponds to a different  $\Delta T$  and error bars indicate the uncertainty in the calculated supersaturation.

### Supersaturation Pressure Dependence with $\Delta T$

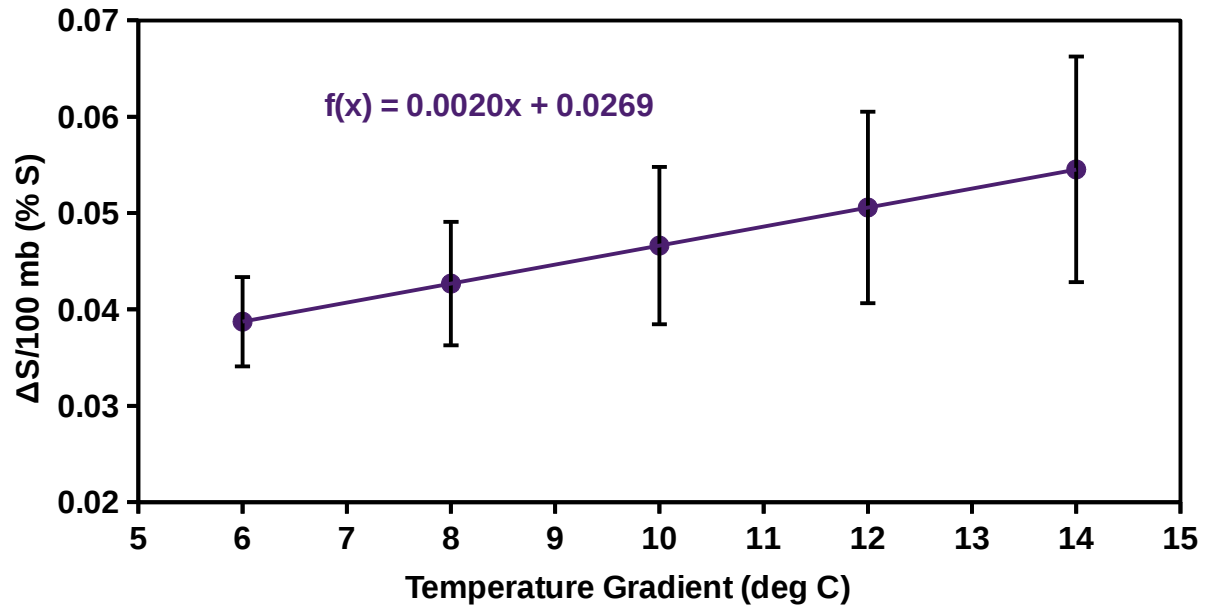


**Figure 13:** Calculated supersaturation pressure dependencies are shown at their corresponding  $\Delta T$  conditions.  $\Delta S$  represents the change in supersaturation percentage. A linear fit is applied to the data to show the relation of the pressure dependence to  $\Delta T$ .

## CHAPTER IV

### DISCUSSION

The DMT CCN counter operator manual advises that the flow calibrations be checked every month. However, when the CCN counter is used in field research the flows are typically calibrated only before a field project. Thus, in order to get a sense of the maximum uncertainty the flow calibrations contribute to the concentration measurements in past field projects, performance checks are conducted on the flow calibrations after a period of 6 months. Therefore, the flow calibration uncertainties found in this research represent the maximum uncertainty of typical observations. Since an uncertainty of 10 % is required to significantly impact measurements and uncertainties in both flow calibrations are below this threshold, the flow calibrations are still valid after 6 months. The uncertainties found in this research represent the conditions SN 062 was exposed to in the lab, so instruments operating in the field could potentially have different uncertainties. The relative deviations in individual points along the supersaturation calibration lines (Figs. 9, 10, and 11) are between 0.1-0.3 % indicating a high level of repeatability using the aforementioned supersaturation calibration methodology. A 2.3-4.4 % uncertainty is found for the supersaturation calibrations with uncertainty increasing as the pressure decreases. Relative deviations of 2.3-4.4 % agree with previous research and with the use of a linear calibration function of supersaturation versus  $\Delta T$  (Rose et al. 2008). Although some error is present, this method proves to be repeatable with relatively low overall error.

As shown in Fig. 12, the supersaturation in the DMT CCN counter depends on pressure.



The dependence of supersaturation on pressure found by Rose et al. (2008) is 0.037 % per 100 hPa at a  $\Delta T$  of 5 K. Rose et al. (2008) also went further to establish a relationship between pressure dependence and  $\Delta T$  in which the relationship is nearly constant, and linear at  $\Delta T$  greater than 6 K. The serial number 062 CCN counter has a similar result as found by Rose et al. (2008) with a pressure dependence of 0.039 % at a  $\Delta T$  of 6 K. Although there is agreement at a similar  $\Delta T$ , this research doesn't examine the lower  $\Delta T$ s ( $\Delta T$  of 2-5 K) used in Rose et al. (2008) that showed significant impacts on the pressure dependence. However, the relationship (Fig. 13) that has been found at  $\Delta T$  greater than 6 K is not constant and a relationship between pressure dependence and  $\Delta T$  can be determined. Although it is nearly constant, the supersaturation pressure dependence ( $100 \text{ hPa}^{-1}$ ) increases as  $\Delta T$  increases by 0.002 % supersaturation  $\text{K}^{-1}$ . The increasing supersaturation pressure dependence with increasing  $\Delta T$  ranges from 0.039 % per 100 hPa at a  $\Delta T$  of 6 K to 0.055 % per 100 hPa at a  $\Delta T$  of 14 K. At  $\Delta T$  higher than 6 K, the pressure dependencies in SN 062 are within 10 % of the pressure dependencies found in Rose et al. (2008). The changing pressure dependence with  $\Delta T$  is most likely caused by the more dramatic changes in water vapor diffusivity at relatively higher temperatures. When the corresponding pressure dependencies at each  $\Delta T$  are averaged, the overall supersaturation dependence on pressure is 0.047 % supersaturation per 100 hPa. Using a single offset ignores the changing supersaturation due to pressure as a function of  $\Delta T$  even though it is a small effect. If a constant supersaturation offset is used to adjust data, it can lead to a corresponding error in supersaturation between 1-4 %. Because the pressure dependence changes over the range of  $\Delta T$ 's, it is more accurate to calibrate the DMT CCN counter at the pressure it will be operating under.

To determine how the uncertainties in the supersaturation and flow rate calibrations affect

concentration measurements, a supersaturation spectrum of outdoor air is used (Fig. 14). At a pressure of 980 hPa, three supersaturation spectra are taken using supersaturations of 0.2, 0.3, and 0.6 %. The uncertainties are applied to the resulting power law equation (Fig. 14) derived from the supersaturation spectrum to determine the percent error of concentration measurements. Based on the supersaturation spectrum and calculated calibration uncertainties, the error in concentration measurements is 8.8, 10.4, and 13.0 % for 700, 840, and 980 hPa respectively. Using these uncertainties, a concentration measurement of 500 #/cm<sup>3</sup> taken at 0.3 % supersaturation and 840 mb becomes 500 ± 52 #/cm<sup>3</sup>. The same 500 #/cm<sup>3</sup> concentration measurement taken at 0.3 % supersaturation and 700 mb becomes 500 ± 65 #/cm<sup>3</sup>. By applying the varying measurement uncertainties with pressure, the magnitude of CCN variability is more quantifiable.

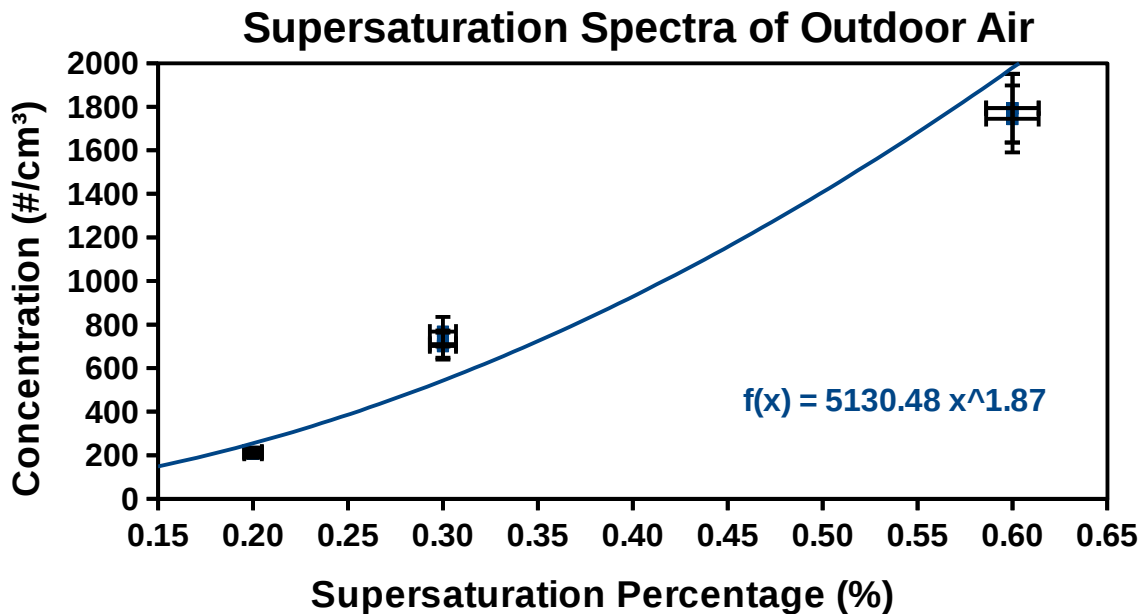


**Figure 14:** Supersaturation spectra (three) of outdoor air at 980 hPa taken with the Droplet Measurement Technologies (DMT) cloud condensation nuclei (CCN) counter on April 7<sup>th</sup>, 2017 in the University of North Dakota Instrumentation Laboratory. A power law fit is applied to the data with the resulting equation being used to describe CCN concentration at a particular supersaturation.

There are large differences between UND calibrations and DMT calibrations on the same instrument. Understanding these differences is essential in determining what methodology to use in future calibrations since it affects comparability among all DMT CCN counter measurements. Fig. 15 shows the disagreement between the DMT and UND calibrations done at the same pressure. The slopes are vastly different leading to supersaturations 42-45 % higher in the DMT calibration than in the UND calibration for the same  $\Delta T$ . Recognizing possible differences in the supersaturation calibration methodology helps to explain why the DMT and UND calibrations differ so much. First, multiply-charged particles can introduce large errors into the calculation of the activation size. Multiply-charged particles pass through the Electrostatic Classifier because their higher charge gives them the same electrical mobility as the smaller particle size being selected. Typically the neutralizer in the Electrostatic Classifier normalizes the random charge distribution of incoming particles to the point where multiply charged particles make up only 0-5 % of all particles being selected in the size selection range of this research. However, given that there is a radioactive element for most neutralizers, radioactive decay decreases the effectiveness of the neutralizer over time. For example, the Kr-85 neutralizer used in this research has a half-life of 10.7 years and the neutralizer (SN 77A-0358) was seven years old at the time of data acquisition. The age of this neutralizer is evident in the activated ratio data as there consistently are plateaus around 4 %. Using a new neutralizer, plateau heights would be expected not to exceed 2 % (Models 3077/3077A Aerosol Neutralizers Instruction Manual, Revision M). While neutralization was not ideal in this research, the amount of error introduced into the activation curves pales in comparison to the error originating from 20-35 % plateaus in the DMT activation curves ( $\Delta T$  3 K for SN 062 calibrated on June 2015).

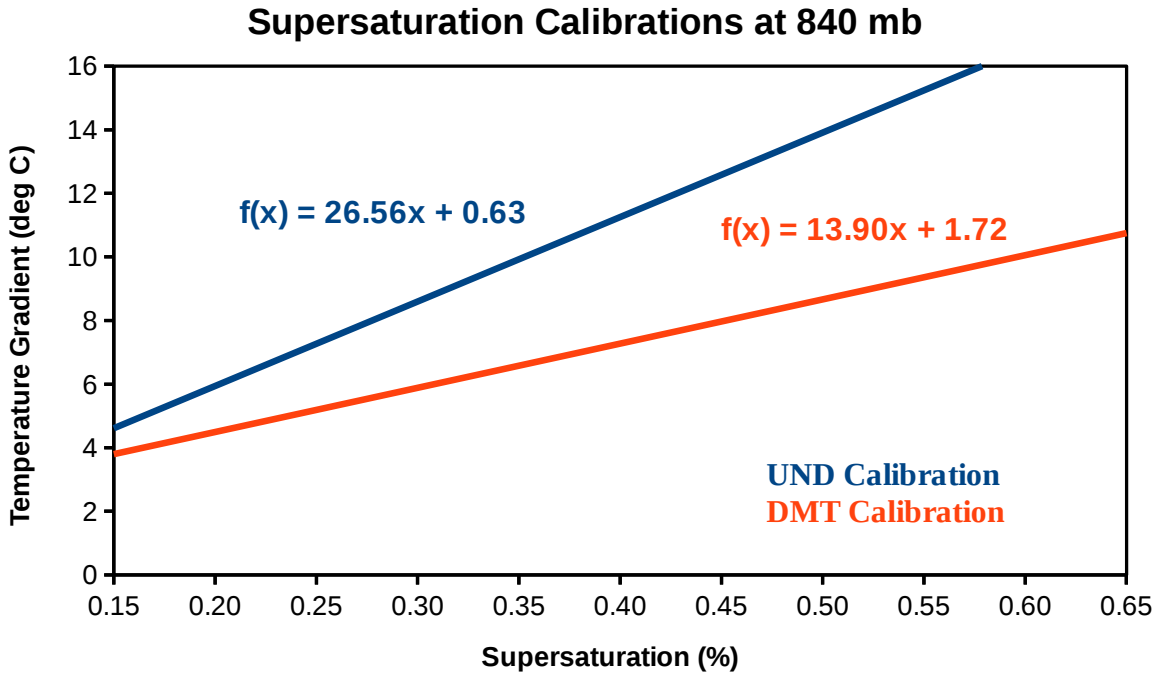


**Figure 15:** Calibration lines for DMT CCN counter SN 062 done at the University of North Dakota and Droplet Measurement Technologies under the same pressure. Calibration equations are displayed in the color of the corresponding calibration line. The UND calibration line was created from data taken between November 17<sup>th</sup>-19<sup>th</sup>, 2016. The DMT calibration line was created using data taken at Droplet Measurement Technologies in August of 2015.

These multiply-charged particles are revealed through a plateau in activated ratio data. The plateaus created by multiply charged particles are indicative of the activation of all multiply-charged particles. Plateau height also represents how much of an influence multiply-charged particles have on the data set as a whole because the fraction of multiply-charged particles observed in the plateau is present throughout the data set. Obtaining the activation size from a data set with a plateau of multiply-charged particles results in a smaller calculated activation size giving a calculated supersaturation higher than the actual supersaturation. Thus, the higher a plateau is, the more the calculated supersaturation is influenced. While there are options for correcting for multiply-charged particles, information about the size distribution of monodisperse particles exiting the Electrostatic Classifier is essential for accurate corrections. Using the

typical calibration methodology, these data are not available. There are other correction options as outlined in Rose et al. (2008), but they require assumptions about the size distribution of monodisperse particles and have inherent errors. If left uncorrected, plateaus that are larger than 0.10 activated ratio cause significant error in calculating activation size. As stated in Chapter III, plateaus below 10 % have been shown to cause no significant decrease in activation size and thus supersaturation percentage ( $< 0.5\%$ ; Rose et al. 2008). Since plateaus in DMT's activated ratio data exceed 10 % ( $\Delta T$  3 K for SN 062 calibrated on June 2015), there is a fairly large amount of error that will be introduced into their calculated activation sizes.

Errors in the supersaturation calibration can also arise from calculating activation size differently. The most accurate methodology requires a sigmoidal curve fit of the activated ratio data to determine the activation size (Rose et al., 2008). However, the DMT CCN counter operator manual (Cloud Condensation Nuclei Counter Operator Manual Revision F, 2004) and calibration data indicate that the activation size is found by linearly interpolating the size at which the activated ratio goes above 50 % after normalization of the data to unity. Normalization to unity, however, has been shown to have little to no effect on calculating activation size ( $< 0.5\%$ ). Also, linear interpolation is erroneous because points on the steep slope of the activation curve have large relative deviations, and not all data are taken into account.

Another influential part of the supersaturation calibration is the Köhler theory used to calculate supersaturation. Different assumptions about parameters in the Köhler equation, particularly about the water activity of the particle, can give relative deviations in calculated supersaturation up to 21 % (Rose et al. 2008). The DMT and UND calibrations use different forms of Köhler theory leading to differences in the calculated supersaturation based on activation size as seen in Fig. 16. The variation of Köhler theory used by DMT leads to

calculated supersaturations approximately 3 % lower at the same activation size throughout an activation size range of 30-140 nm.

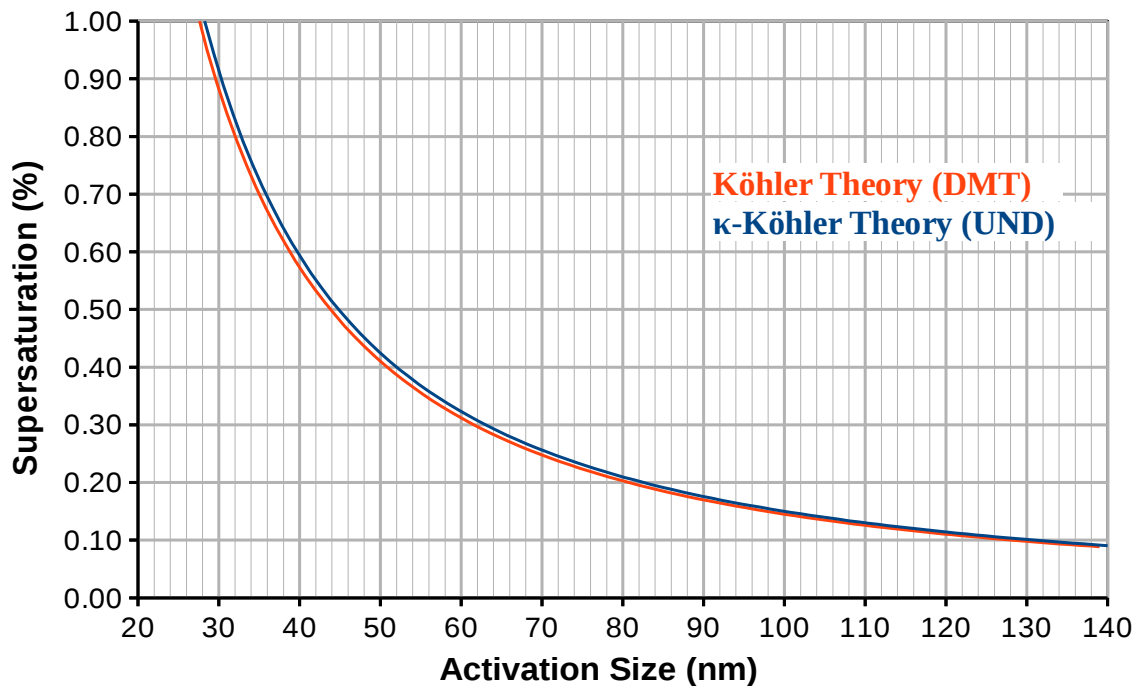


**Figure 16:** Comparison of DMT variation of Köhler theory and kappa-Köhler theory calculated supersaturations based on activation sizes for ammonium sulfate. Kappa-Köhler theory includes a parameterization of water activity based on the chemical composition of measured particles. Labels are colored according to their corresponding Köhler curve.

An additional potential error source that may account for the difference between DMT and UND calibrations relates to assumptions made about the chemical composition of the calibration aerosols. The UND calibration uses a kappa value of 0.61 corresponding to pure ammonium sulfate. Contamination can influence kappa, however, which can impact activation significantly. For the calibrations in this research, the atomizer, dryer, mixing box, classifier and all lines (Figure 3) were cleaned prior to calibration. Furthermore, pure ammonium sulfate was dissolved in ultrapure water, meaning that the amount of dissolved solids (contaminants) is negligible. Thus, the chemical composition of the aerosols used in this research is known to a high degree of certainty.

Another possible element leading to major differences in the UND and DMT calibrations are differences in the  $\Delta T$ 's used for calibration. The DMT calibration uses four  $\Delta T$ 's between 3 and 8 K, while the UND calibration uses five  $\Delta T$ 's between 6 and 14 K. The supersaturation calibration function is not linear below 0.1 % (Roberts and Nenes, 2005), and a  $\Delta T$  of 3 K corresponds to a supersaturation around 0.1 %. Supersaturations of 0.1 % and lower have been found to deviate around 40 % from the supersaturation calibration line (Rose et al., 2008). Previous research has not investigated whether or not this non-linearity stays at 0.1% over time, so it is possible that the point at which the supersaturation calibration function changes from linear to non-linear can move due to changes inside the instrument. Regardless, calibrating the instrument at points near to where the calibration function is no longer viable can potentially influence the entire calibration function's slope. The combination of large plateaus in activation curves, incorrect fitting methods, questionable calibration conditions, and different Köhler theory variation leads to the supersaturation differences of 42-45 % between the two different calibrations.

## CHAPTER V

### CONCLUSION

The DMT CCN counter is calibrated at reduced pressure which is important for deployment on research aircraft where the usage of a constant pressure inlet is required. The relative uncertainties of the supersaturation are between 0.1-0.3 % indicating a very repeatable method. The uncertainties in the supersaturation calibration are 2.3, 3.1, and 4.4 % for 980, 840, and 700 hPa pressure conditions respectively, which is very close to the 3 % found by other experiments (Rose et al., 2008). The supersaturation decreases an average of 0.047 % supersaturation for every 100 hPa decrease in pressure. The slope of the supersaturation calibration line increases 5.4 % per 100 hPa decrease in pressure. The slope change is a result of the changing pressure dependence with changing  $\Delta T$ , amounting to an increasing pressure dependence ( $100 \text{ hPa}^{-1}$ ) of 0.002 % supersaturation  $\text{K}^{-1}$ . The changing pressure dependence agreed within 10 % of the change found by Rose et al. (2008). The general conclusion that can be drawn from the uncertainty and pressure dependence calculations is that while conditions can be reasonably accounted for when adjusting a DMT CCN counter calibration, it is best to calibrate the instrument at the counter's operating pressure. Rose et al. (2008) confirm this as they concluded they recommend careful calibration under relevant conditions during every field campaign to ensure reliable operation.

Although many of the conclusions reached by this study are confirmed by previous research, information about the effects of the uncertainties on concentration measurements has



not previously been explicitly defined. The uncertainties introduced from the flow rate and supersaturation calibrations can affect the concentration measurements of the CCN counter by up to 8.8, 10.4, and 13.0 % at 980, 840, and 700 hPa respectively. A significant advantage of the methodology used in this research is that the calibrations performed at reduced pressure were done at a single location using a constant pressure inlet. Another study used simulated aircraft conditions to conduct calibrations (Roberts et al. 2010), but this research has gone further to investigate the uncertainties associated with calibrating under reduced pressures.

In addition to conclusions on the instrument's uncertainty and supersaturation pressure dependence, insight is gained on the importance of calibration methodology for the supersaturation calibration of the DMT CCN counter. UND supersaturation calibrations were found to be 42-45 % lower than those performed at DMT less than a year prior. These differences primarily reside in the calibration methodology followed by the two groups. Multiply-charged aerosols and fitting methods were found to be potential sources of error. It is also likely that the different  $\Delta T$ 's used by DMT and UND led to a large part of the slope difference in the respective supersaturation calibration lines. Since the goal of this research is to aid in the comparability of measurements it should be noted that the supersaturation calibration is not trivial and proper methodology must be used to maintain comparability.

The relative uncertainties found indicate a very repeatable calibration methodology under simulated aircraft conditions in the laboratory. Supersaturation calibration uncertainties increase with decreasing pressure, and a supersaturation pressure dependence is defined. To achieve the most accurate results the DMT CCN counter should be calibrated at its operating pressure using proper methodology.

## Appendix A

### Data Processing

Several steps are taken to produce calibration lines for the DMT CCN counter after raw data has been collected. Raw data from the CCN counter are logged in a .csv file. The data file is first converted from .csv to the standard NASA text file format (outlined in the ADPAA software package documentation, Delene et al. 2011) using the 'process\_day\_dmtccnc' script. Similarly, the raw data from the CPC are converted to the standard NASA text file format using the 'convert\_cpc3771tonasa' script. Both of the aforementioned scripts have an option to apply a time offset which is calculated to determine the delay in the air sample reaching either the CPC or DMT. Another NASA text file is manually created from lab book documentation to define start and end times for dry particle sizes being selected in the DMA. The time interval file, CPC text file, and DMT text file are then combined using the 'CCNCactivationsize' script. 'CCNCactivationsize' calculates the average counts and standard deviation in each instrument encompassed by the defined time interval for each generated particle size. The script then calculates the activated ratio as well as the standard deviation for the sample at each time interval. The file generated by 'CCNCactivationsize' is fed into the script 'sigmoidfit' to create activation curves using the curve\_fit fitting routine in SciPy 18.1. As long as the first ratio point is known to be approximately zero ( $< 0.01$ ), it is weighted heavily to avoid large influence of plateaus on the rest of the curve. After generating an activation curve, 'sigmoidfit' will output the activation size based on the half point between the maximum and minimum of the ratio data. The activation size given by 'sigmoidfit' is placed into a text file along with instrument pressure and Delta T for supersaturation calculations. The script, 'SScal' is used to calculate the supersaturation percentage based on the activation size using Kappa- Köhler theory. Finally,

'SScal' creates the calibration line plots as well as an output file containing the standard deviations and calibration coefficients.

## Appendix B

### Condensation Particle Counter Theory of Operation

The TSI model 3772 Condensation Particle Counter (CPC) is a continuous flow, diffusional, alcohol-based, thermal-cooling condensation nuclei counter. It can detect particles as small as 10 nm in diameter. Below 10 nm in diameter the detection efficiency drops below 50%. The instrument operates similar to an optical particle counter where it measures the scattering of light by droplets to count each individual droplet. In order to count the sub-micron sized particles, however, the particles must be enlarged through condensation of vapor onto them (CPC Operator Manual p. 59). What makes this counter different from an optical particle counter is its ability to condense vapor onto the particles to count them.

In order to condense vapor onto the particles the instrument creates supersaturated conditions inside the instrument using butanol. Since butanol is a more volatile compound than water, using butanol allows particles to condense and grow under temperature conditions inside the instrument that are easy to manage. The aerosol stream, which is pulled into the instrument at  $1.0 \text{ L min}^{-1}$  by an external vacuum pump, passes through a heated saturator block at  $39 \text{ C}^{\circ}$  (CPC Operator Manual p. 43). Here, butanol vapor evaporates and saturates the aerosol stream (CPC Operator Manual p. 63). Butanol is replenished into the saturator block from a reservoir inside the instrument and a fill bottle. The instrument checks the liquid level in the reservoir every ten minutes and if it is below a threshold, the instrument pulls more butanol into the reservoir from the fill bottle. The aerosol stream then passes through the relatively cool condenser at  $22 \text{ C}^{\circ}$  where the aerosol stream is supersaturated with respect to butanol at a saturation ratio of several hundred percent. The high supersaturation in the condenser allows the butanol to condense onto the particles in the aerosol stream where the diameter increases rapidly

to a detectable size (CPC Operator Manual p. 63). It should be noted, however, that the instrument is designed to function under ambient temperatures of 10 to 35 C° (CPC Operator Manual p. 43). Temperatures outside this range can affect the instrument's ability to create the proper supersaturation inside the condenser, which is critical.

When butanol vapor reaches a certain supersaturation around the particles, it will begin to condense onto the particles. However, if supersaturation is too high, then condensation of the vapor can occur without any particles present. This phenomenon is known as homogeneous nucleation. In order to avoid homogeneous nucleation occurring in the counter, the temperatures are accurately controlled to maintain a supersaturation below that required for homogeneous nucleation (CPC Operator Manual p. 59). At a particular saturation ratio, defined as vapor partial pressure divided by the saturation vapor pressure at a given temperature, vapor will condense onto particles as a function of the size of the particles. The Kelvin diameter gives the minimum size a particle must be to act as a condensation nucleus at a particular supersaturation and is expressed by the following equation (CPC Operator Manual p. 60):

$$S = \frac{P}{P_s} = \exp\left(\frac{4\gamma M}{\rho RTd}\right), (1)$$

where  $\gamma$  is surface tension of the condensing fluid,  $M$  is the molecular weight of the condensing fluid,  $\rho$  is the density of the condensing fluid,  $R$  is the universal gas constant,  $T$  is the absolute temperature, and  $d$  is the Kelvin diameter. This equation presents the relationship that a higher saturation ratio leads to a lower Kelvin diameter. And in this instrument, the operating supersaturation is set via the saturator and condenser temperatures so that particles 10 nm in diameter and larger act as condensation nuclei and grow. An important note, however, is that the saturation vapor pressure is defined for a planar surface of liquid. For a curved surface such as a

droplet, where curvature increases with decreasing radius, it is easier for molecules to escape the liquid surface (CPC Operator Manual p. 60). This is because the curvature decreases the magnitude of intermolecular forces keeping the molecule in liquid. Thus the saturation vapor pressure error, though not significant, increases with decreasing drop diameter.

When grown droplets pass from the condenser through a nozzle into the optical detector block, the laser light shown on the aerosol stream is scattered by the grown droplets. Using a pair of aspheric lenses, the scattered light is focused onto a low-noise photodiode which then senses each grown droplet as it passes through the beam. The housing of the optics is kept at a steady 40 C° to avoid condensation on the sensing components (CPC Operator Manual p. 63).

Some potential problems that can arise with the CPC are flooded optics and leaks. In order to check for leaks in this instrument, a conventional vacuum leak checker cannot be used as this can pull butanol onto the lenses and flood the optics. A high efficiency filter must be placed ahead of the CPC to check for leaks. If the instrument is not counting zero particles, then there is either a leak or the optics are flooded (CPC Operator Manual p. 97). A leak will show as relatively constant counts on the CPC whereas flooded optics will present as counts that fluctuate rapidly over a wide range. Possible leak sources for the CPC include anything directly connected to the inlet tube. Inside the instrument there are a series of o-rings around the inlet tube where the tube connects into the saturator block, ventilation, and pressure sensor lines. Over time these o-rings can wear out and it is important to check these if a leak is identified. Another potential leak point is where the inlet tube connects to take samples in front of the instrument. If metal ferrules are used to connect the sample tube, the end can get warped over time and cause a leak (CPC Operator Manual p. 32). Leaks must be minimal if not, nonexistent, because under lower pressures they can become severe. This can contaminate data to a point

where they are unusable.

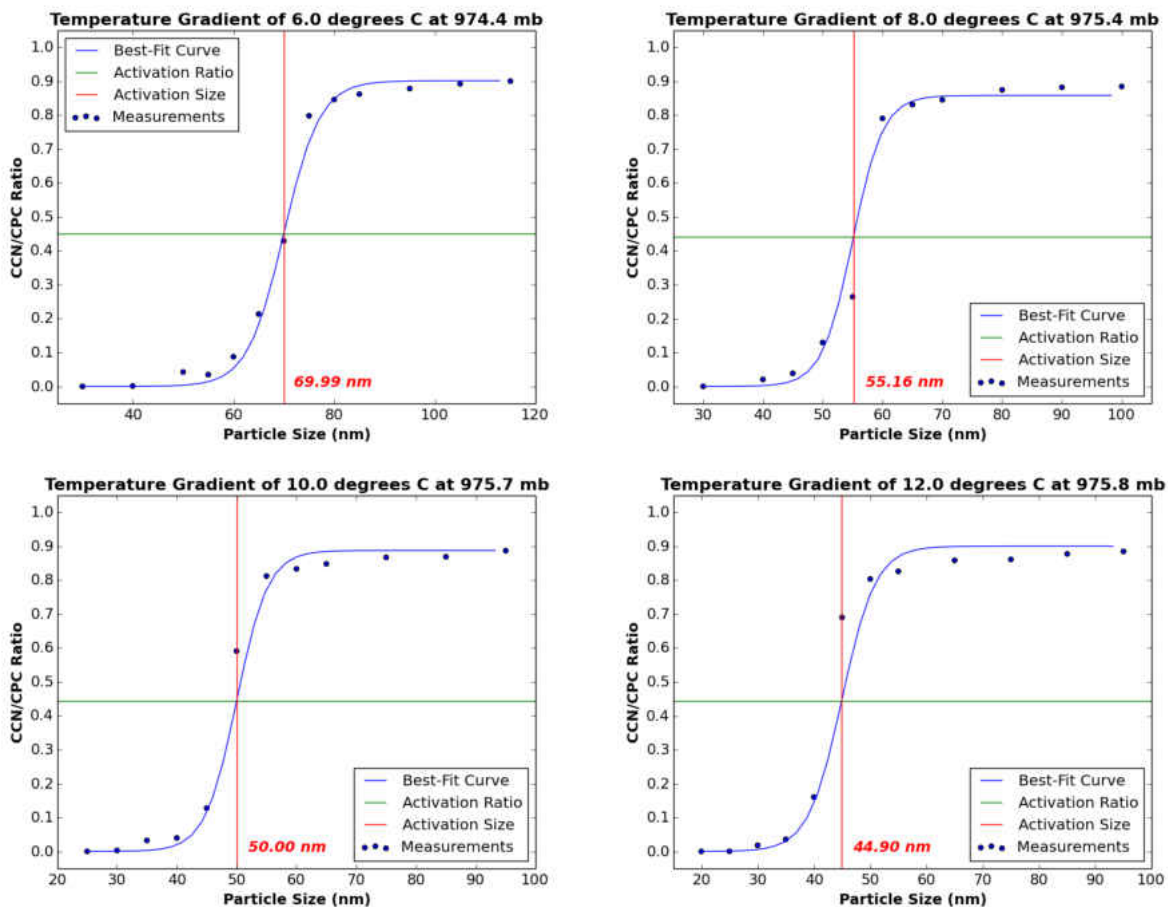
If the CPC has flooded optics it has most likely pulled against a vacuum. When the CPC pulls against a vacuum butanol gets pulled into the aerosol line at uncontrolled concentrations and deposits onto the lenses in the optical detector block. This distorts the scattering of light greatly and particle counts randomly fluctuate over a wide range (CPC Operator Manual p. 95). Maintaining an awareness of the CPC theory of operation is essential in understanding and preparing the instrument to perform at lower pressures.

## Appendix C

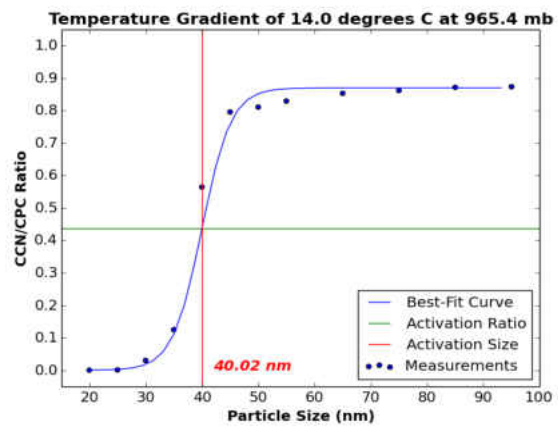
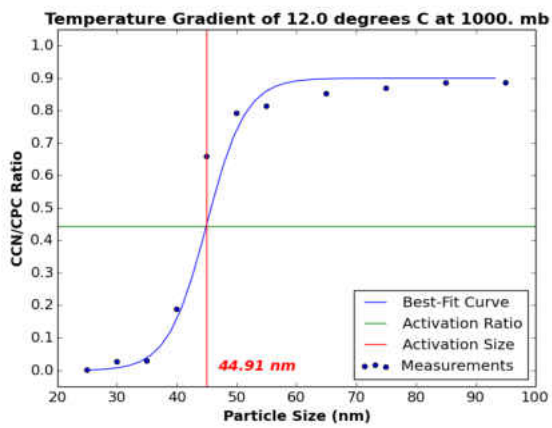
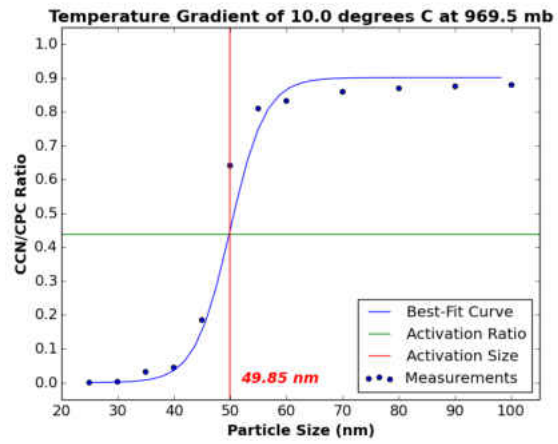
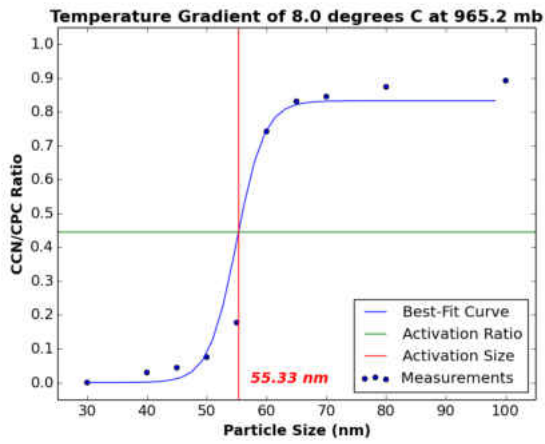
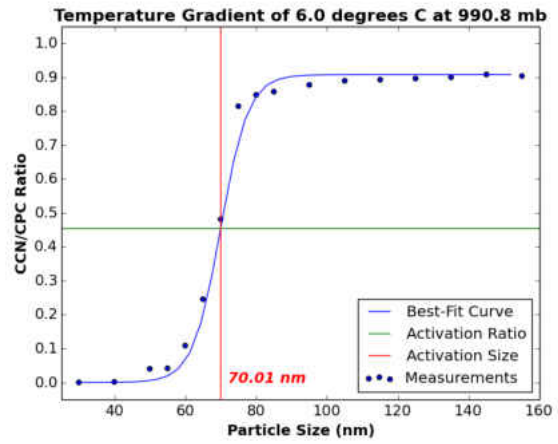
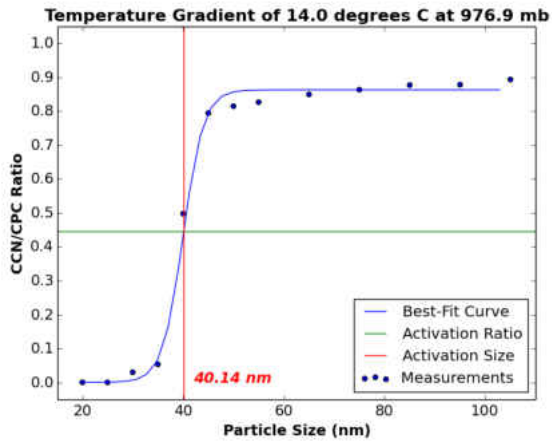
### Activation Curves Generated for Supersaturation Calibrations

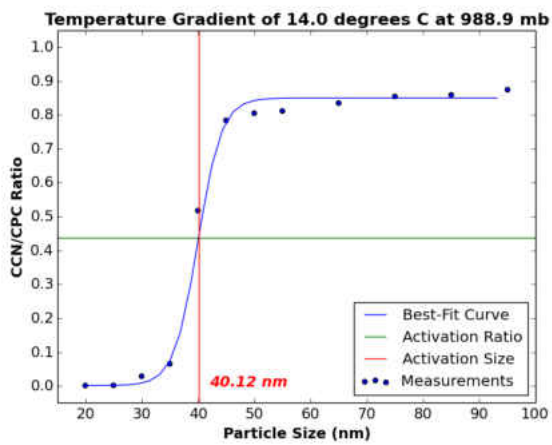
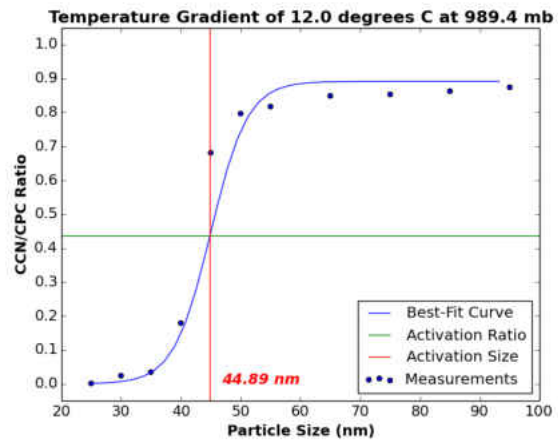
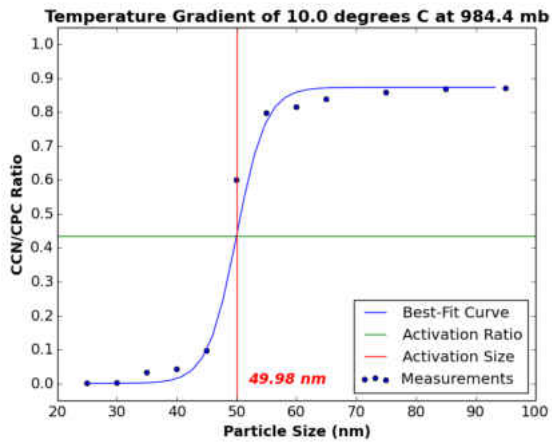
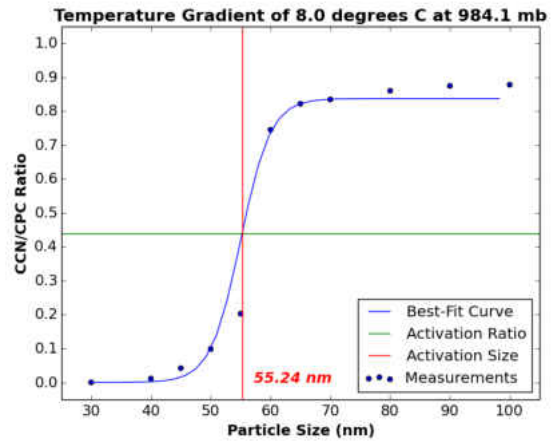
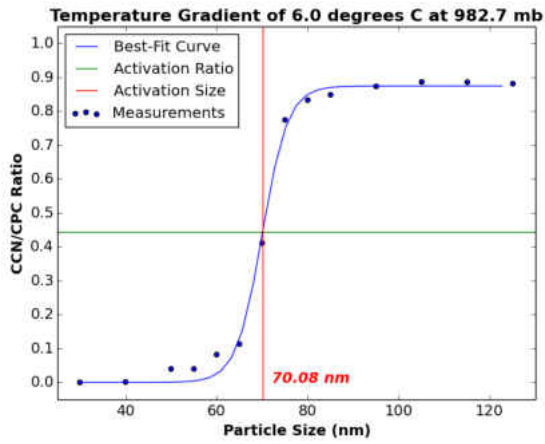
Shown below are all activation curve fits of measured ratio data taken between October 28<sup>th</sup> and November 19<sup>th</sup>, 2016 in the University of North Dakota Instrumentation Laboratory. Each section shows the activation curves generated for calibrations performed at pressure levels of 980, 840, and 700 hPa. Three activation curves are generated at each  $\Delta T$  between 6 and 14 K at each pressure level. The data are fitted with a sigmoidal curve using the Python SciPy curve\_fit module. The activation size is represented by the red vertical line, as well as displayed in red italicized text. The activation ratio is represented by the horizontal green line.

#### 980 hPa Activation Curves

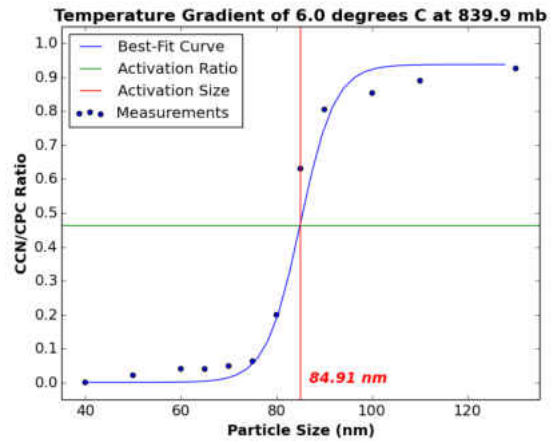
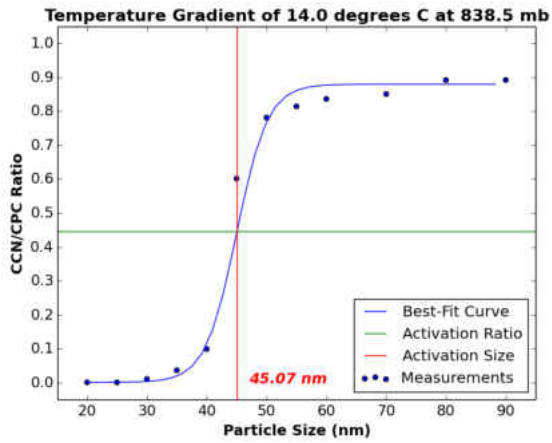
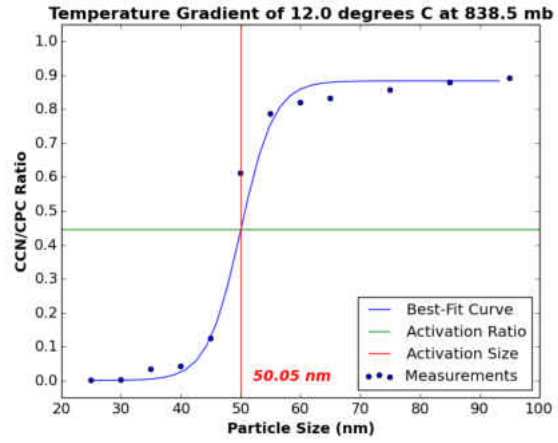
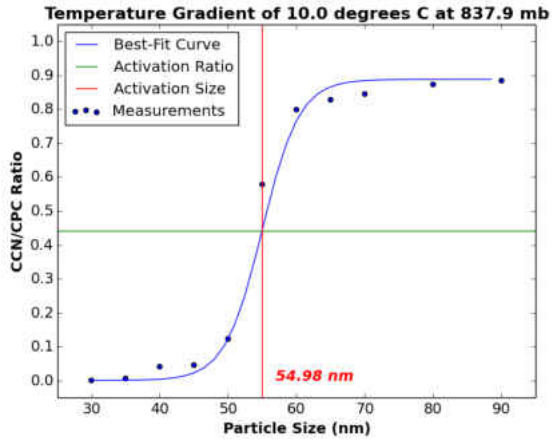
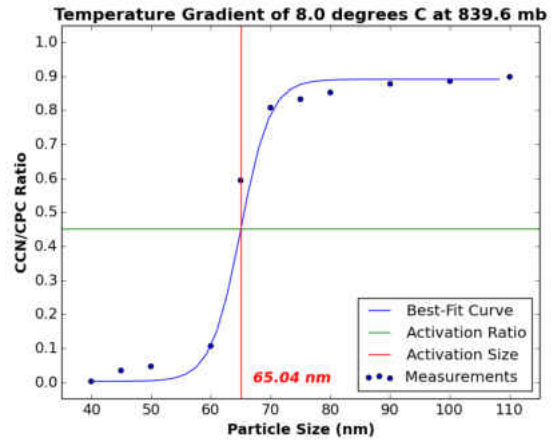
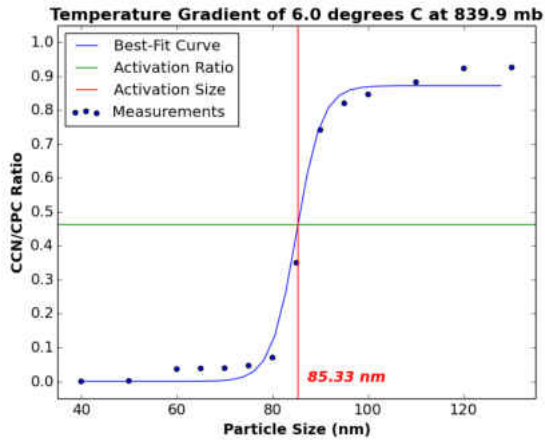


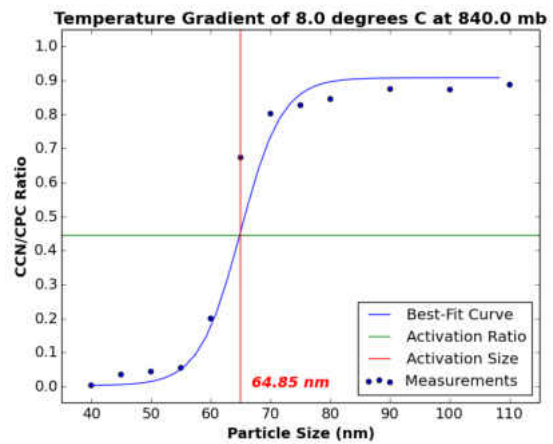
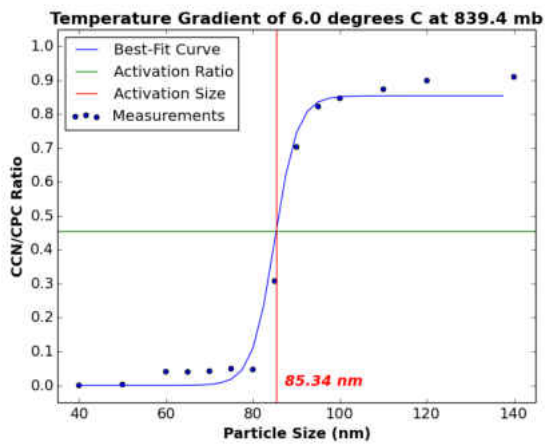
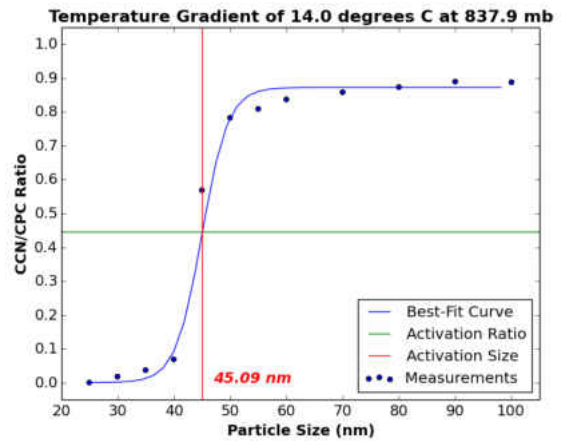
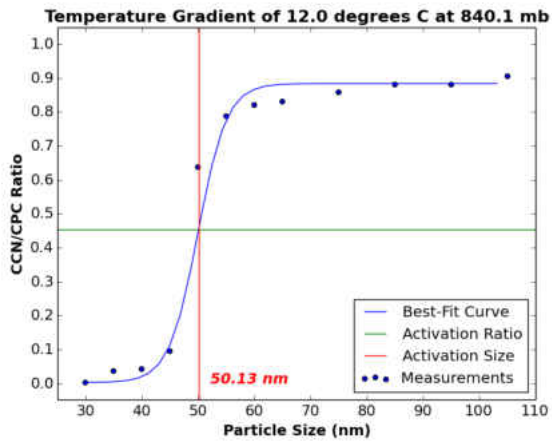
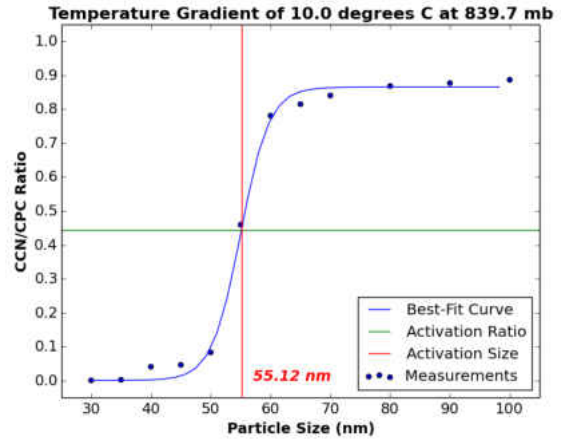
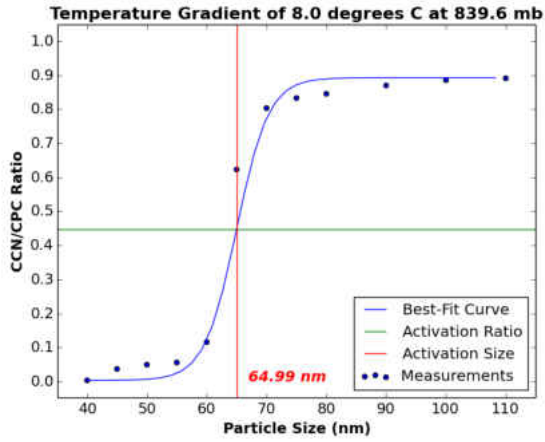


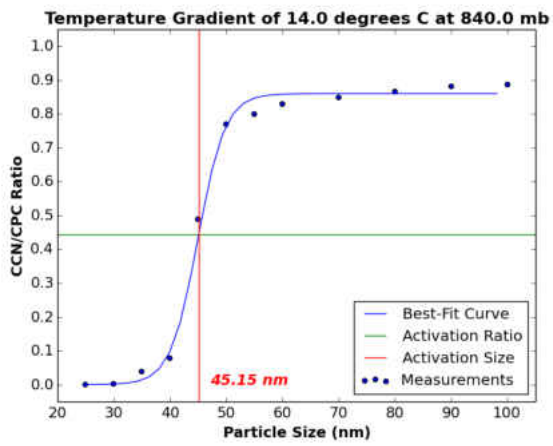
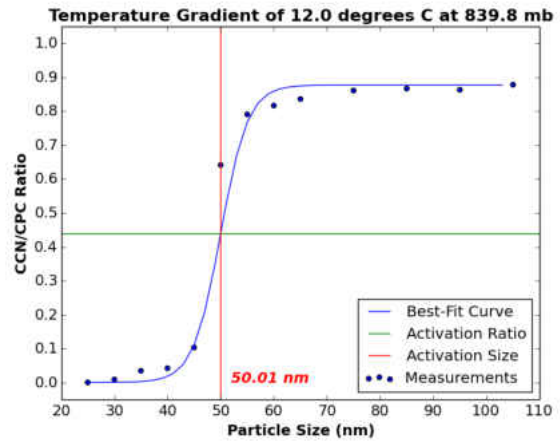
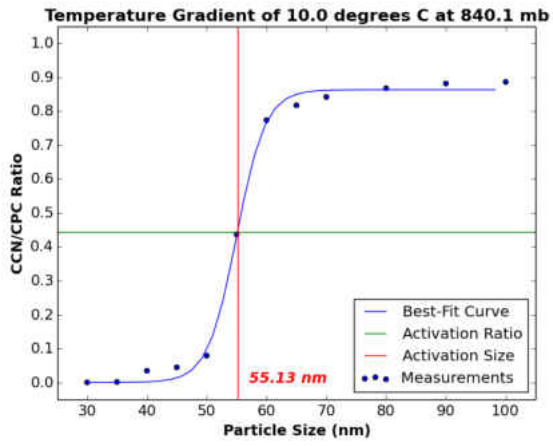




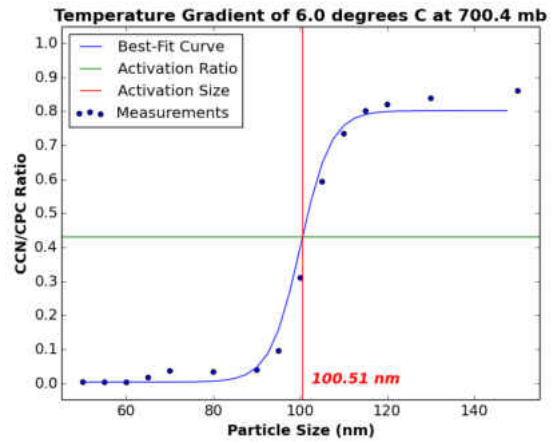
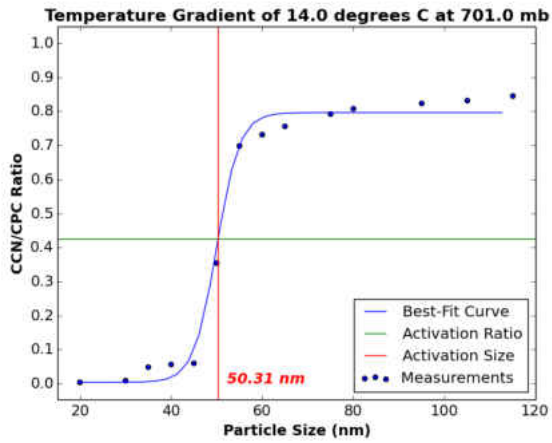
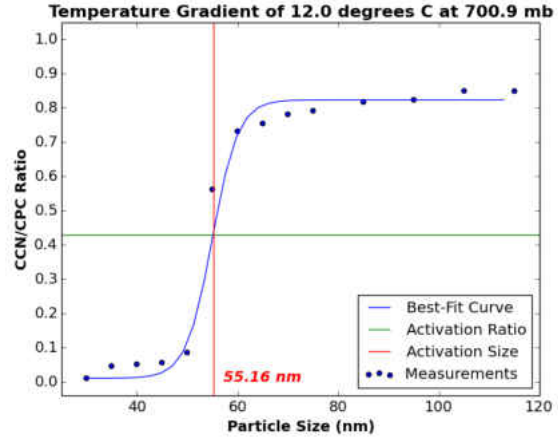
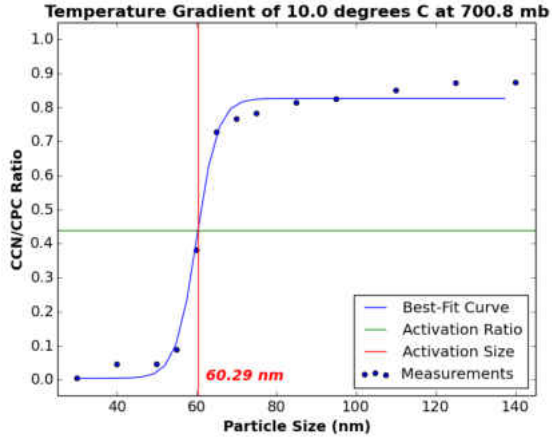
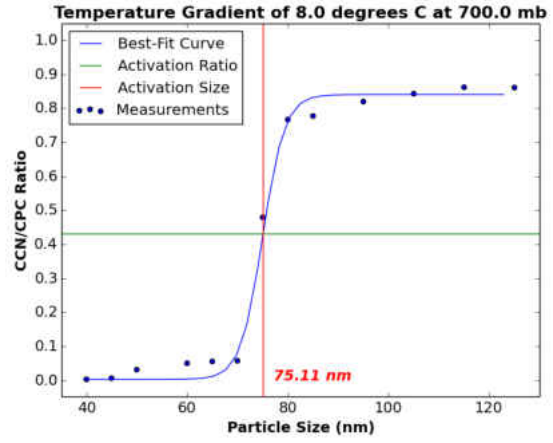
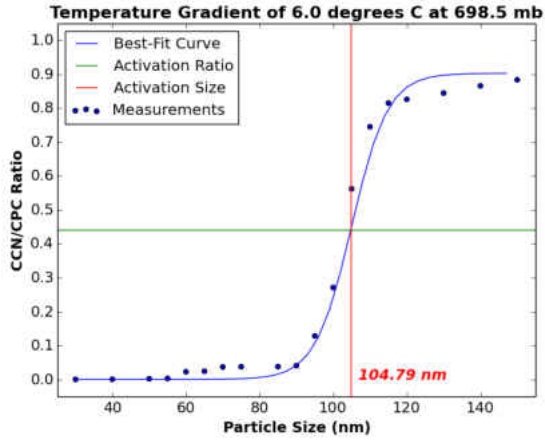
# 840 hPa Activation Curves

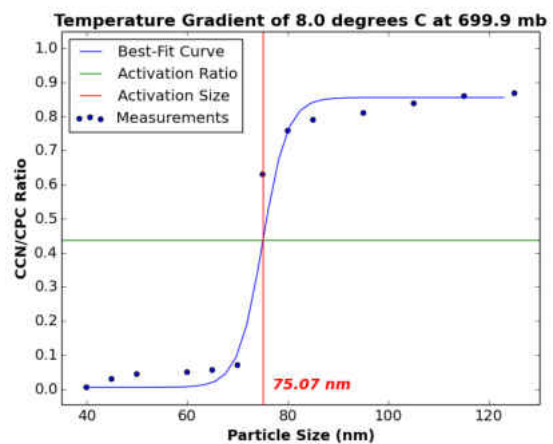
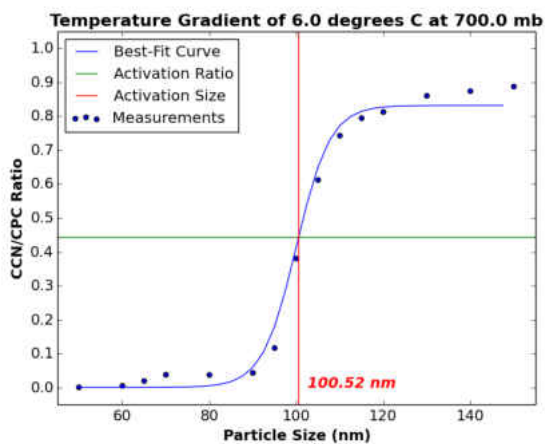
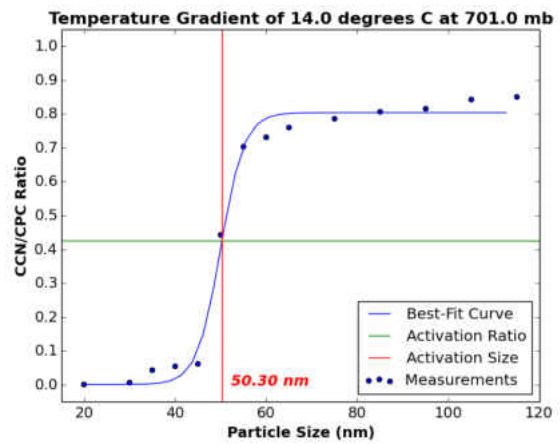
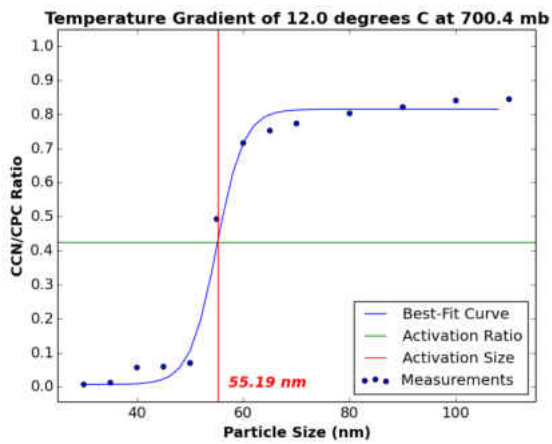
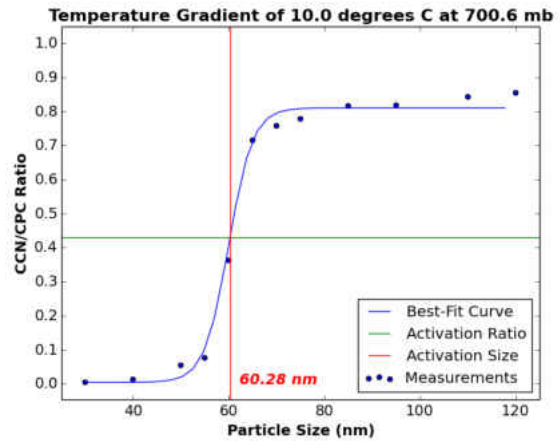
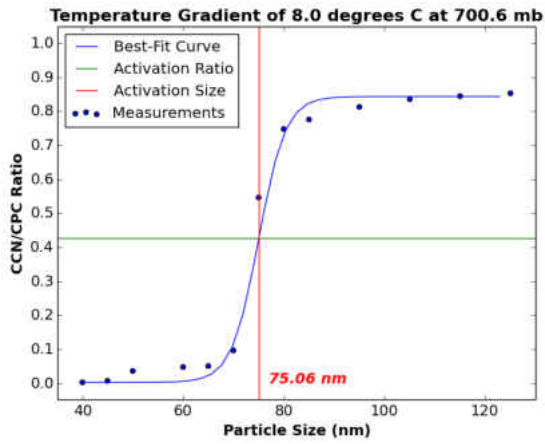


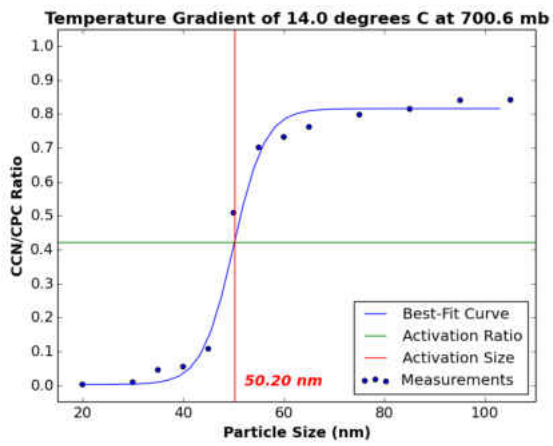
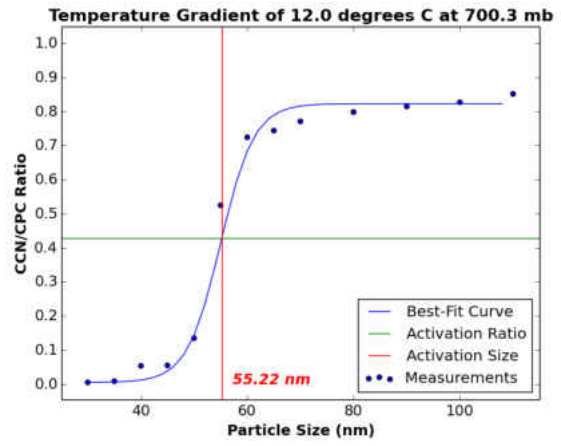
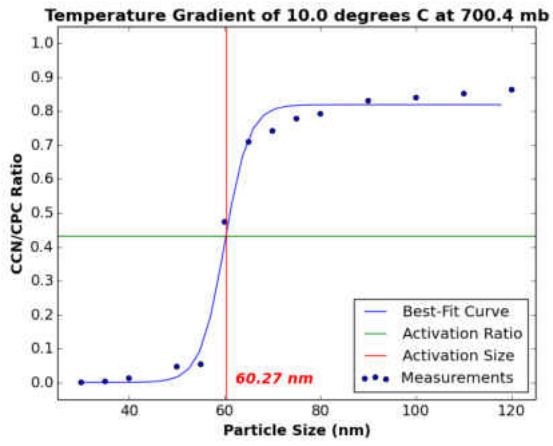




# 700 hPa Activation Curves









## REFERENCES

- Alofs, D.J. and T. Liu, 1981: Atmospheric measurements of CCN in the supersaturation range 0.013–0.681%. *J. Atmos. Sci.*, **38**, 2772–2778, doi:10.1175/1520-0469(1981)038<2772:AMOCIT>2.0.CO;2.
- Delene, D. J., Airborne Data Processing and Analysis Software Package, Earth Science Informatics, **4(1)**, 29-44, 2011, doi:10.1007/s12145-010-0061-4.
- Droplet Measurement Technologies Inc., 2004: Cloud Condensation Nuclei Counter Operator Manual. S/N: 062 DOC-0086 Revision F, 86 pp.
- Forster, P., and Coauthors, 2007: Changes in Atmospheric Constituents and in Radiative Forcing, *Fourth Assessment Report of the Intergovernmental Panel on Climate Change*. United Kingdom: Cambridge University Press.
- Gunthe, S. S., and Coauthors, 2009: Cloud condensation nuclei in pristine tropical rainforest air of Amazonia: size-resolved measurements and modeling of atmospheric aerosol composition and CCN activity, *Atmos. Chem. Phys.*, **9**, 7551-7575, doi:10.5194/acp-9-7551-2009.
- Horvath, H., R. L. Gunter, and S. W. Wilkison, 1990: Determination of the coarse mode of the atmospheric aerosol using data from a forward-scattering spectrometer probe, *Aerosol Sci. Technol.*, **12:4**, 964-980, doi:10.1080/02786829008959407.
- Hudson, J.G., 1989: An instantaneous CCN spectrometer. *J. Atmos. Oceanic Technol.*, **6**, 1055–1065, doi:10.1175/1520-0426(1989)006<1055:AICS>2.0.CO;2.
- Hudson, J.G., 1993: Cloud condensation nuclei. *J. Appl. Meteor.*, **32**, 596–607, doi:10.1175/1520-0450(1993)032<0596:CCN>2.0.CO;2.
- Hudson, J.G. and P. Squires, 1973: Evaluation of a recording continuous cloud nucleus counter. *J. Appl. Meteor.*, **12**, 175–183, doi:10.1175/1520-0450(1973)012<0175:EOARCC>2.0.CO;2.
- Hudson, J.G. and P. Squires, 1976: An Improved Continuous Flow Diffusion Cloud Chamber. *J. Appl. Meteor.*, **15**, 776–782, doi:10.1175/1520-0450(1976)015<0776:AICFDC>2.0.CO;2.
- IPCC, 2014: *Climate Change 2014: Mitigation of Climate Change. Contribution of Working Group III to the Fifth Assessment Report of the Intergovernmental Panel on Climate Change*.

Edenhofer, O., and Coauthors. Cambridge University Press, Cambridge, United Kingdom and New York, NY, USA.

Lance, S., and Coauthors, 2009: Cloud condensation nuclei activity, closure, and droplet growth kinetics of Houston aerosol during the Gulf of Mexico Atmospheric Composition and Climate Study (GoMACCS), *J. Geophys. Res.*, **114**, D00F15, doi:10.1029/2008JD011699.

Lee, L. A., K. J. Pringle, C. L. Reddington, G. W. Mann, P. Stier, D. V. Spracklen, J. R. Pierce, and K. S. Carslaw, 2013: The magnitude and causes of uncertainty in global model simulations of cloud condensation nuclei, *Atmos. Chem. Phys.*, **13**, 8879-8914, doi:10.5194/acp-13-8879-2013.

Lindsey, D. T., and M. Fromm, 2008: Evidence of the cloud lifetime effect from wildfire-induced thunderstorms, *Geophys. Res. Lett.*, **35**, L22809, doi:10.1029/2008GL035680.

Moore, R. H., and A. Nenes, 2009: Scanning flow CCN analysis—a method for fast measurements of CCN spectra, *Aerosol Sci. Technol.*, **43:12**, 1192-1207, doi: 10.1080/02786820903289780

Petters, M. D. and S. M. Kreidenweis, 2007: A single parameter representation of hygroscopic growth and cloud condensation nucleus activity, *Atmos. Chem. Phys.*, **7**, 1961-1971, doi:10.5194/acp-7-1961-2007.

Pierce, J. R. and P. J. Adams, 2009: Uncertainty in global CCN concentrations from uncertain aerosol nucleation and primary emission rates, *Atmos. Chem. Phys.*, **9**, 1339-1356, doi:10.5194/acp-9-1339-2009.

Roberts, G. C. and A. Nenes, 2005: A continuous-flow streamwise thermal gradient CCN chamber for atmospheric measurements, *Aerosol Sci. Technol.*, **39:3**, 206-221, doi: 10.1080/027868290913988.

Roberts, G. C., D. A. Day, L. M. Russell, E. J. Dunlea, J. L. Jimenez, J. M. Tomlinson, D. R. Collins, Y. Shinozuka, and A. D. Clarke, 2010: Characterization of particle cloud droplet activity and composition in the free troposphere and the boundary layer during INTEX-B, *Atmos. Chem. Phys.*, **10**, 6627-6644, doi:10.5194/acp-10-6627-2010.

Rose, D., S. S. Gunthe, E. Mikhailov, G. P. Frank, U. Dusek, M. O. Andreae, and U. Pöschl, 2008: Calibration and measurement uncertainties of a continuous-flow cloud condensation

nuclei counter (DMT-CCNC): CCN activation of ammonium sulfate and sodium chloride aerosol particles in theory and experiment, *Atmos. Chem. Phys.*, **8**, 1153-1179, doi:10.5194/acp-8-1153-2008.

Saponaro, G., P. Kolmonen, L. Sogacheva, E. Rodriguez, T. Virtanen, and G. de Leeuw, 2017: Estimates of the aerosol indirect effect over the Baltic Sea region derived from 12 years of MODIS observations, *Atmos. Chem. Phys.*, **17**, 3133-3143, doi:10.5194/acp-17-3133-2017.

Sinnarwalla, A.M. and D.J. Alofs, 1973: A cloud nucleus counter with long available growth time. *J. Appl. Meteor.*, **12**, 831-835, doi:10.1175/1520-0450(1973)012<0831:ACNCWL>2.0.CO;2.

TSI Inc., 2003: Models 3077/3077A Aerosol Neutralizers Instruction Manual. P/N 1933077 Revision M, 123 pp.

TSI Inc., 2005: Model 3076 Constant Output Atomizer Instruction Manual. P/N 1933076 Revision J, 63 pp.

TSI Inc., 2006: Series 3080 Electrostatic Classifiers Operation and Service Manual. P/N 1933792 Revision G, 145 pp.

TSI Inc., 2007: Model 3772/3771 Condensation Particle Counter Operation and Service Manual. P/N 1980529 Revision C, 127 pp.

Twomey, S., 1974: Pollution and the planetary albedo, *Atmos. Environ.*, **41**, 120-125, doi:10.1016/j.atmosenv.2007.10.062.

Weidensohler, A., 1988: An approximation of the bipolar charge distribution for particles in the submicron size range, *J. Aerosol Sci.*, **19**, 387-389, doi:10.1016/0021-8502(88)90278-9.